A developmental requirement for HIRA-dependent H3.3 deposition revealed at gastrulation in Xenopus.

Emmanuelle Szenker, Nicolas Lacoste, Geneviève Almouzni

A developmental requirement for HIRA-dependent H3.3 deposition revealed at gastrulation in *Xenopus*

Emmanuelle Szenker [1,2], Nicolas Lacoste [1,2] and Geneviève Almouzni [1,2,*]

[1] Institut Curie, Centre de Recherche, Paris, F-75248 France

[2] CNRS, UMR218, Paris, F-75248 France

* Corresponding author

Phone: 33 (0) 1 46 27 67 01

Fax: 33 (0) 1 46 33 30 16

Email: almouzni@curie.fr

Running Title: Developmental role of H3.3 and its chaperone HIRA

SUMMARY

How histone variants that mark distinct chromatin regions impact a developmental program is a major challenge in the epigenetics field. To assess the importance of the H3.3 histone variant and its dedicated histone chaperone HIRA, we used an established developmental model, *Xenopus laevis*. Following the early rapid divisions exploiting a large maternal pool of both replicative H3.2 and replacement H3.3, H3.3 transcripts show a distinct peak of expression at gastrulation. Depletion of both H3.2 and H3.3 leads to an early gastrulation arrest. However, with only H3.3 depletion, defects occur at late gastrulation, impairing further development. Providing exogenous H3.3, but not replicative H3.2 mRNAs, rescues these defects. Notably, downregulation of the H3.3 histone chaperone HIRA similarly impairs late gastrulation and we find a global defect in H3.3 incorporation into chromatin comparable to H3.3 depletion. We discuss how specific HIRA-dependent H3.3 deposition is required for chromatin dynamics during gastrulation.

HIGHLIGHTS

- H3.3 transcription peaks at gastrulation
- Lack of H3.3 expression impairs *Xenopus* development at late gastrulation
- The H3.3 chaperone HIRA is also required for late gastrulation
- HIRA-dependent H3.3 deposition is required during development

INTRODUCTION

Proper packaging of eukaryotic DNA into chromatin is required for functional genome organization (Probst et al., 2009). This involves the use of a fundamental motif, the nucleosome, which comprises DNA wrapped around histones. A large number of variations, including covalent post-translational modifications (PTMs) of histones (Jenuwein and Allis, 2001; Turner, 2002), and histone variant incorporation (Ahmad and Henikoff, 2002b; Boyarchuk et al., 2011; Loyola and Almouzni, 2007; Sarma and Reinberg, 2005) defines distinct chromatin landscapes typical of individual cell types.

In mammals, several H3 variants contribute to these landscapes including the replicative forms H3.1 and H3.2, the replacement variant H3.3, and the centromere-specific H3 variant CenH3 (CENP-A) (Szenker et al., 2011). While the unique importance of CENP-A for defining the identity of the centromere is well documented, the respective roles of the closely related H3 replicative forms compared to the replacement variant H3.3 are less clear. The expression of replicative H3 peaks in S phase to supply histones during DNA replication. In contrast, the replacement variant H3.3, which is expressed throughout the cell cycle, in quiescent cells, and during distinct stages of differentiation, provides a continuous source of histones (Szenker et al., 2011). Thus, given the overall similarity of the core particle containing either type of histone H3 (Tachiwana et al., 2011), one might assume that these subtypes could functionally substitute for one another and that incorporation of distinct replicative or replacement H3 is mainly due to their availability during the cell cycle.

However, H3.3 is specifically enriched within regions of high transcriptional activity (Ahmad and Henikoff, 2002a; Chow et al., 2005; Jin and Felsenfeld, 2006; Jin et al., 2009; Mito et al., 2005; Schwartz and Ahmad, 2005) and typically marked by

PTMs associated with active transcription such as H3K4 methylation (Hake et al., 2006; Loyola et al., 2006; McKittrick et al., 2004; Waterborg, 1990). This prompted the hypothesis that H3.3 could mark transcriptionally active genes, potentially by promoting transcription and/or as a consequence of transcription. The dynamic properties of tagged H3.3 nucleosomes, revealed by their unusual sensitivity to salt-dependent disruption could account for an enhancement in transcriptional activity (Jin and Felsenfeld, 2007). Interestingly, based on nuclear transfer and reprogramming experiments in *Xenopus laevis,* the memory of an active state is thought to involve H3.3 maintenance through a number of cell divisions without ongoing transcription (Ng and Gurdon, 2008). Indeed, the observed maintenance of H3.3 is unlikely to involve reactivation of transcription at each cycle, given that zygotic transcription only starts after the twelfth division in *Xenopus* (Newport and Kirschner, 1982). Furthermore, the global incorporation of maternal H3.3 onto male DNA upon fertilization in *Drosophila* (Loppin et al., 2005) and mice (Torres-Padilla et al., 2006; van der Heijden et al., 2005) underlines the capacity of this histone to be incorporated independently of transcription. Obviously, these findings emphasize a major requirement of H3.3 for reproduction in both organisms, but do not address the question of its importance at later stages during development.

A further comparison of H3.3 function during development in several organisms (Banaszynski et al., 2010; Orsi et al., 2009; Szenker et al., 2011) highlights the fact that developmental roles of H3.3 are still poorly defined. In *Drosophila*, most animals with mutations of both H3.3 genes survive to adulthood and appear morphologically normal but are sterile (Hodl and Basler, 2009; Sakai et al., 2009), most likely due to a deficiency in protamine replacement by maternal H3.3 onto male DNA at fertilization (Loppin et al., 2005). In mice, a hypomorphic mutation

in only one of the two H3.3 genes leads to unexplained neonatal lethality in 50% of cases. Yet surviving animals show not only subfertility phenotypes but also growth and neuromuscular defects (Couldrey et al., 1999). Subfertility phenotypes could reflect defects in paternal genome reprogramming since alteration in protamine replacement by H3.3 is critical for promoting heterochromatin formation (Santenard et al., 2010). However, other growth defects suggest additional developmental roles in vertebrates. Most recently, in human, the observations of somatic mutations affecting H3 variants or their chaperones in specific pediatric tumors further emphasize the importance of considering their role in a developmental context (Schwartzentruber et al., 2012; Wu et al., 2012).

Our choice of *Xenopus laevis* as an ideal model system to reveal novel aspects of H3.3 function was guided by four important criteria. Firstly, the fact that *Xenopus* sperm chromatin, unlike *Drosophila* and mice, retains H3 variants and H4 histones (Katagiri and Ohsumi, 1994)**,** enables us to examine H3.3 developmental roles separately from protamine replacement. Secondly, the presence of a single representative of the replicative H3 in *Xenopus*, related to human H3.2, makes the situation simpler to analyze. Thirdly, the relatively high level of H3.3 transcripts in early development compared to adult tissues, as noted in global gene expression analyses (Baldessari et al., 2005), suggested additional developmental roles for H3.3. Finally, powerful *in* vitro assays using *Xenopus* egg extracts permit the study of specific histone deposition pathways, involving dedicated histone chaperones (Ray-Gallet and Almouzni, 2004).

Indeed, much has been elucidated concerning histone H3 variants' dynamics and their specific chaperones (De Koning et al., 2007). For replicative H3, Chromatin Assembly Factor 1 (CAF-1), which comprises three subunits, namely p150, p60 and

p48, represents the major candidate for deposition in a DNA synthesis-dependent manner (Smith and Stillman, 1989; Tagami et al., 2004). Concerning H3.3, the early identification of HIRA as a histone chaperone promoting H3.3 deposition onto DNA *in vitro* using extracts derived from *Xenopus* eggs (Ray-Gallet et al., 2002; Tagami et al., 2004), made it the first candidate for this role *in vivo*. In *Drosophila,* HIRA functions together with the remodeling factor Chromodomain Helicase DNA-binding protein 1 (CHD1) to promote H3.3 loading onto male DNA during sperm decondensation (Konev et al., 2007; Loppin et al., 2005). However, other H3.3 histone chaperones have been recently identified in mammals, including a complex composed of the death-associated protein (DAXX) and the alpha-thalassemia/mental retardation X-linked syndrome protein (ATRX) (Drané et al., 2010; Goldberg et al., 2010; Lewis et al., 2010). The recent analysis of *de novo* histone H3 incorporation in cultured cells using the SNAP tagging system advanced the notion that the HIRA deposition pathway could work at any time during the cell cycle to ensure chromatin integrity whenever a failure in histone deposition occurs (Ray-Gallet et al., 2011). How such a requirement may become critical during the development of a whole organism has yet to be established.

In this paper, we studied H3.3 during *Xenopus* development and found that it is required for late gastrulation to proceed. Importantly, this requirement cannot be substituted by replicative H3.2. Similarly, the HIRA chaperone proved critical at late gastrulation, and HIRA morphants showed chromatin defects associated with reduced H3.3 levels and higher sensitivity to MNase digestion. We discuss how HIRA-mediated H3.3 deposition is required to meet the needs of chromatin dynamics to properly complete gastrulation in *Xenopus*.

RESULTS

H3.3 is specifically required during gastrulation

We first explored the expression profile of H3 variants both at the RNA and protein levels during *Xenopus* development. We found both by Northern blot and *in situ* hybridization that transcripts corresponding to both variants are maternally stored in the egg with a distinct peak for H3.3 at gastrulation (Figure S1A and S1B). This was complemented by our analysis at the protein level using a Triton Acetic acid Urea (TAU) gel (Zweidler, 1978), which shows that both H3.2 and H3.3 are present at similar levels in eggs through the Mid Blastula Transition (MBT) stage (Figure S1C), suggesting an equal use of both maternal proteins prior to MBT. After this transition, H3.3 protein levels decreased relative to H3.2 to reach a level comparable to that in somatic cells, where the replicative H3 largely dominates as observed in HeLa cells (Loyola et al., 2006). These observations prompted us to explore whether H3.3 could have a particular contribution at the time of gastrulation during *Xenopus* early development. To address the functional importance of H3 proteins, we designed specific antisense morpholino oligonucleotides that prevent translation of target transcripts when injected into embryos. We first tested our morpholinos (MO) for specificity in oocytes (not shown) and then assessed their efficiency in embryos. Using soluble fractions derived from embryos injected with the respective morpholinos, we show that MO H3.3 specifically diminishes H3.3 while MO H3 targets both H3.2 and H3.3 (Figure 1A). This is shown by Western Blot analysis using monoclonal antibodies whose specificity for either H3.2 or H3.3 was confirmed (Figure S2A). In MO H3 treated embryos, we observed an early gastrulation developmental arrest (Figure 1B and Movie S1). This is consistent with the prevention of all new H3 expression while exhausting the maternal histone proteins

(Laskey et al., 1978). Of note, this arrest is comparable to a CAF-1 p150 MO (Figure S2B), and occurs later than the one observed when a dominant negative form of CAF-1 interferes with chromatin assembly prior to the MBT in *Xenopus* (Quivy et al., 2001). In contrast, the specific knockdown of H3.3 enabled further developmental progression in early gastrulation but revealed later defects (Figure 1B and Movie S1). Embryos surviving to the tailbud stage show severe developmental defects including an open blastopore, *spina bifida* and a shortened antero-posterior axis (Figure 1B – white arrow). The penetrance and severity of the phenotype was dose-dependent (Figure S3A), but never matched the effect seen with the morpholino targeting both H3.2 and H3.3 (MO H3). Closer inspection revealed a slowdown of morphogenetic movements leading to embryos that failed to close their blastopore correctly at the end of gastrulation and that shed cells through the open blastopore (Figure 1B, Movies S1 and S2).

To ask whether this gastrulation phenotype simply reflects a general limitation in availability of H3 or is specifically due to H3.3 loss, we designed a rescue experiment by injecting MO H3.3 together with control GFP, H3.2-HA or H3.3-HA mRNAs (Figure 2C). First, we verified that both H3.2 and H3.3 tagged constructs could be effectively incorporated into chromatin (Figure 2A). Moreover, to eliminate the possibility that depletion of the variants may affect the chaperones, we documented the expression of the H3.2 and H3.3 histone chaperones, CAF-1 and HIRA, in the embryos throughout development (Figure S3B), and verified that they remain unaffected in gastrulae upon downregulation of H3.3 (Figure 2B). These data establish that both tagged H3.2 and H3.3 are functional, and that depletion of H3.3 does not affect H3-specific chaperones. The observation of embryos at the early tailbud stage (stage 25) revealed a rescue in 62% of MO H3.3 treated embryos with

the co-injection of H3.3 transcripts, supporting the specificity of the observed phenotype (Figure 2B). Notably, co-injection of H3.2 mRNAs failed to rescue gastrulation defects in H3.3-deficient embryos (Figure 2B). Comparable protein levels for GFP, H3.2, and H3.3 in injected embryos confirmed that the lack of rescue could not reflect a defect in H3.2 mRNAs translation (Figure 2C). Taken together, our data support a model where there is a specific requirement for H3.3 for proper gastrulation that cannot be bypassed by H3.2 overexpression.

H3.3-mediated defects at gastrulation and abnormal expression of late mesoderm markers

Among the important events occurring during gastrulation, mesoderm induction represents a major developmental step that involves activating the expression of a series of genes. The induction starts at stage 9.5, and accumulation of specific transcripts is diagnostic of a successful process. As a reference, we first examined the gene *Xenopus* brachyury (Xbra), a transcription factor whose transcripts mark the marginal zone, a region containing cells destined to become mesoderm, at the gastrula stage (stage 11) (Herrmann and Kispert, 1994; Showell et al., 2004). Following injection with MO H3.3 in one cell of 4 cell-stage embryos, we found by *in situ* hybridization that Xbra expression is clearly reduced at gastrulation and throughout development when H3.3 is depleted (Figure 3A - white arrows, Figure S3C). We thus conclude that H3.3 is critical for the proper expression of a mesodermal gene, Xbra.

We then analyzed a larger series of lineage marker genes by RT-qPCR after depletion of H3.3 in embryos harvested at stage 11 (Figure 3B and S4A). First, we considered genes involved in early mesoderm induction, which are in part

responsible for Xbra expression (Heasman, 2006), including genes encoding TGFβ factors such as Derrière or proteins of the nodal family (*Xenopus* nodal related genes, Xnrs). For a comparison, we also examined transcription factors involved in endoderm formation such as Sox17, Mixer and Mix1 (Heasman, 2006). We found that the expression level of endodermal genes and mesodermal-inducing factors such as Xnr2 and Derrière did not significantly change in H3.3 morphant embryos when compared to control embryos (Figure 3B and S4A). We then examined the expression of genes directly implicated in the formation of the mesodermal layer, including Xbra, eFGF, xWnt11, Myf5 and MyoD (Heasman, 2006). Importantly, we confirmed the defect in Xbra expression levels, in parallel with the downregulation of eFGF, Wnt11, Myf5 and MyoD (Figures 3B and S4A and B). This is in accordance with the facts that eFGF and Xbra cross-activate each other's expression during the establishment of the mesoderm (Isaacs et al., 1994) and that MyoD expression is regulated by eFGF and Xbra (Fisher et al., 2002). Taken together, our data show that while early mesoderm inducing signals are largely unaffected, abnormal expression of later mesodermal differentiation markers occurs in H3.3 morphants.

Interestingly, we found both by RT-qPCR and *in situ* hybridization that H3.3 downregulation also affects the expression of some genes implicated in the dorsal neural regulatory network including Chordin, ADMP and the downstream pro-neural genes Otx2 and Sox2 (Heasman, 2006), but not Sip1, a known inhibitor of Xbra (Lerchner et al., 2000; Verschueren et al., 1999) (Figure S4A and B). However, ventral pro-epidermal genes such as xVent1 and xVent2 were not significantly affected (Figure S4A). These data support a model whereby loss of H3.3 impacts a set of genes that should normally be activated during mesoderm and neuroectoderm induction in the embryos at a similar time. This phenotype could potentially be due to

either a defect in the mesoderm and/or neuroectoderm induction signals to specifically activate target genes, or, alternatively, it may be a consequence of the fact that activated genes at this particular stage become more dependent on H3.3 for the maintenance of their expression.

H3.3 is dispensable for initiation of mesoderm-induction yet critical for cell viability

To test the hypothesis whereby the mesoderm induction would be impaired in H3.3 morphants, we employed animal cap assays to investigate whether H3.3 morphants could respond to exogenous mesoderm-inducing factors. Using activin as a mesoderm-inducing growth factor to stimulate animal cap elongation (Suzuki et al., 1994), we did not observe a statistically meaningful difference between H3.3 morphants and controls when treating animal caps either for 90 minutes (Figure 4A – 5ng) or 24 hours (data not shown). This is in contrast to the dramatic effect observed with the dominant negative form of Xbra, Xbra-EnR (Conlon et al., 1996) (Figure 4A and Figure S5A). Interestingly, when we increased the amount of MO H3.3 to try to exacerbate a potential elongation defect, the animal caps instead disintegrated (Figure 4A – 9.2ng). When examining H3.3 morphants more closely at the end of gastrulation, we observed white cells shed outside the embryos, a first indication of cell death (Figure 4B and Movie S2). We confirmed cell death in H3.3 morphants both at the gastrula and neurula stages (in contrast to control embryos, Figure 4C) by a Terminal deoxynucleotidyl transferase dUTP Nick End Labeling (TUNEL) assay detecting DNA fragmentation (Hensey and Gautier, 1997). Taken together, our data show that in an animal cap assay using exogenous activin, the early response to mesoderm induction does occur in H3.3 morphants, but ultimately a strong depletion

leads to cell death. These data indicate that early events can take place, but maintenance of the activation is impaired and downregulation of H3.3 leads to cell death when gastrulation fails to progress.

HIRA is required for loading H3.3 and late gastrulation

We then asked whether the requirement for H3.3 could relate to a specific need for H3K4 methylation, given that this mark is specifically enriched on H3.3 nucleosomes that accumulate at actively transcribed loci. Global levels of H3K4 methylation are severely reduced when the highly conserved WD40-repeat protein 5 (WDR5), a major methyl K4-associated factor, is downregulated in *Xenopus* embryos (Wysocka et al., 2005), leading to developmental defects in tadpoles (Figure S5B). However, WDR5 knockdown embryos did not show any gastrulation defects resembling H3.3 downregulation (Figure 5B) and Xbra transcription was unaffected (Figure 5C). Thus, the requirement for H3.3 at gastrulation cannot relate directly to H3K4 methylation promoted by WDR5.

We then assessed whether loss of HIRA could disrupt *Xenopus* development in a manner comparable to H3.3. Injection of morpholinos specifically downregulating HIRA proteins in embryos (Figure 5A) led to late gastrulation defects similar to the ones observed in H3.3-deficient embryos (Figure 5B – white arrows, Figure S3A for different doses of MO). In addition, *in situ* hybridization of HIRA morphants showed a comparable downregulation of Xbra (Figures 5C and S3C). We conclude that HIRA plays a critical role during late gastrulation in a manner that resembles the H3.3 requirement. This parallel suggested a possible connection between HIRA and H3.3 deposition that warranted further exploration.

Interestingly, *in vitro* nucleosome assembly assays using *Xenopus* egg extracts supported a critical role for HIRA in a deposition pathway independent of DNA synthesis using depletion experiments (Ray-Gallet et al., 2002) and as shown here by neutralization with antibodies (Figure 6A). We thus tested if HIRA morphants showed defects in their chromatin particularly with respect to H3.3 incorporation. Given the comparable phenotypes between H3.3 and HIRA morphant embryos, an interdependency between them had to be considered. We thus compared their chromatin status in parallel, and found that in both H3.3 and HIRA morphants, the amount of H3.3 in the chromatin is similarly affected (Figure 6B). We thus showed a direct and major impact of HIRA on H3.3 *in vivo*. Furthermore, the analysis of chromatin sensitivity to MNase digestion in H3.3 or HIRA morphants showed remarkable similarity in its increased digestion relative to control embryos (Figure 6C). Taken together, these data support a view where HIRA is necessary to ensure H3.3 deposition and this would be critical at the time of gastrulation. We thus propose that a mechanism involving HIRA for H3.3 deposition, independent of DNA synthesis, is critical at the time of gastrulation.

DISCUSSION

Our data in *Xenopus* demonstrate the unique importance of the H3.3 variant at gastrulation, a critical transition during vertebrate development marked by major changes in cell cycle and developmental programs. Importantly, while the morpholino approach in *Xenopus* could unveil a time when H3.3 first becomes critical, other stages of development and cell differentiation could equally require H3.3 deposition. Thus, these findings should be considered with a broad implication.

A distinct role for H3.3 at late gastrulation

Remarkably, the distinct late gastrulation defects arising after depletion of H3.3 with morpholinos could not be overcome by providing exogenous H3.2 mRNAs. Thus, the two types of H3 variants are not easily interchangeable at this critical developmental stage. This argues for a specific requirement for H3.3 and/or its deposition mode rather than a mere histone H3 gene dosage deficiency. Similarly, in *Tetrahymena,* extra provision of replicative H3 cannot overcome the absence of H3.3 (Cui et al., 2006) and H3.3A knock-out mice are neonatal lethal (Couldrey et al., 1999). Intriguingly, though sterile, most *Drosophila* embryos lacking H3.3 survive until adulthood. However this involves an upregulation of the replicative histone H3 transcripts to compensate for the lack of H3.3 (Hodl and Basler, 2009; Sakai et al., 2009). It is thus possible that the overexpression of one variant in the absence of the other enables *Drosophila* embryos to survive. This would support the view that the variant itself may not be the most critical parameter but it would rather be the ability to exploit different deposition pathways and corresponding chaperones.

The impact of H3.3 on transcriptional program at late gastrulation

Here, following depletion of H3.3, clear defects occur at late gastrulation with a failure of blastopore closure and increased cell death. Importantly, the expression of nodal-related genes, which are fundamental for both mesoderm and endoderm formation in early gastrula embryos (Watabe and Miyazono, 2009), were unaffected by the lack of H3.3. Thus, the importance of H3.3 does not equally impact simply any transcribed gene, but rather relates to their activation timing. This is consistent with the downregulation after H3.3 depletion of the mesodermal marker, Brachyury (Xbra), one of the many genes controlled by the nodal/activin signaling pathway (Latinkic et al., 1997). In addition to Xbra and eFGF, we also found that Myf5, as well as a downstream master gene in muscle differentiation, MyoD, are also downregulated. In agreement with these observations, a recent report showed that H3.3 histone deposition occurs at the MyoD promoter in a cellular model reproducing myogenic transcriptional activation (Yang et al., 2011). This could reflect a direct impact of H3.3 on transcription as proposed (Elsaesser et al., 2010), as well as the necessity to incorporate more H3 outside S phase when these genes are transcribed. These two possibilities are not mutually exclusive, and each should be considered. The presence of H3.3 at regions with high histone turnover, including promoters and regulatory elements (Goldberg et al., 2010; Ray-Gallet et al., 2011), could contribute to maintaining particular settings. In particular, in the context of chromatin changes during early development in *Xenopus*, other histone variants (Almouzni et al., 1994; Dimitrov et al., 1993) should be considered, especially given the crosstalk between H3.3 and H2A.Z promoting transcription in cellular models (Jin and Felsenfeld, 2007). First, somatic H1, whose overexpression reduces mesoderm-specific MyoD induction during gastrulation (Steinbach et al., 1997; Vermaak et al., 1998), could antagonize H3.3, as suggested by the anticorrelation between H1 and H3.3 distribution genome-

wide (Braunschweig et al., 2009). Second, H2A.Z, whose depletion in *Xenopus laevis* led to gastrulation defects (Ridgway et al., 2004), could function together with H3.3 to antagonize H1 and establish permissive chromatin settings. These specific chromatin settings, beyond having an impact on transcriptional maintenance, could also contribute to maintaining chromatin integrity and thereby impact cell viability.

The importance of a HIRA-dependent H3.3 deposition pathway to establish/maintain specific chromatin states

The critical requirement of H3.3 may reflect the need for histone incorporation to replace histones at any sites presenting chromatin defects/nucleosome disruption (De Koning et al., 2007). Recent findings showed that HIRA could enable nucleosomal free DNA to be reassembled genome wide when the CAF-1-dependent deposition of replicative H3 failed (Ray-Gallet et al., 2011). During gastrulation, when the length of gap phases are becoming significant, replicative chromatin assembly will not suffice to re-establish proper chromatin organization, and this may become even more critical at highly induced gene loci (Newport and Kirschner, 1982). A decrease in nucleosome density beyond a threshold could lead to cell death, possibly through mitotic catastrophe. While we could show that H3.3 was critically required during development, it was important to consider histone chaperones as an important aspect of histone variant dynamics (De Koning et al., 2007). Downregulation of HIRA proved critical during late gastrulation in our experiments in a manner paralleling the defects upon H3.3 downregulation. This is illustrated not only at the developmental level, but most importantly at the chromatin level, where we could detect decreased H3.3 levels and increased sensitivity to MNase digestion, similar to direct H3.3 depletion. Thus, we provide here a clear interdependency in the embryo between

HIRA and H3.3, which both affect chromatin at a global level. Further studies will be needed to determine how the complex histone chaperone network acts with H3.3 during development.

Conceptually, the fact that a mechanism acting at the chromatin level and linked to cell cycle can both integrate changes in transcription and help maintain a transcriptional program provides an ideal regulatory means during normal development to control the balance between cell differentiation and viability. In pathological situations where H3 variants are mutated (Schwartzentruber et al., 2012; Wu et al., 2012), it will be important these requirements to elucidate their contribution to tumor progression.

EXPERIMENTAL PROCEDURES (for details, see supplemental information)

Embryo manipulation

We prepared embryos as in (Almouzni et al., 1994; Roche et al., 2006) and staged them according to (Nieuwkoop and Faber, 1967). Procedures for the animal cap assay (Green, 1999) involved dissecting animal caps from stage 8 embryos, and incubating with Activin (R&D systems, catalog #338-AC-010, 5ng/mL) for 90 minutes, followed by transfer in Activin-free medium for further incubation until sibling embryos had reached the neurula stage. Assays for terminal deoxynucleotidyl Transferase dUTP Nick End Labeling (TUNEL) on embryos were performed as described (Hensey and Gautier, 1997).

Whole mount in situ hybridization

We performed whole-mount RNA *in situ* hybridizations (WISH) as described (Sive et al., 2000). We revealed using BM purple substrate (Roche Diagnostics) and acquired images with a LEICA MZ FLIII stereomicroscope. When indicated, we performed cross sections on fixed embryos before the *in situ* hybridization experiment. See extended experimental procedures for details on plasmids and probes.

Morpholino and mRNA microinjection

We microinjected embryos using a Drummond Nanoject injector (Drummond Scientific, Broomall, PA, USA) with an injection volume set from 4.6 to 27.6nL to deliver the appropriate quantity of MO or mRNA (as indicated). See Table S1 for MO sequences (Gene Tools, LLC) that anneal to the initiation region (start codon) of

targeted mRNAs; see supplemental information for details on *in vitro* transcribed specific 5' capped mRNAs.

Protein extracts preparation and Western blotting

We prepared total protein extracts from embryos using the CelLytic Express reagent (Sigma-Aldrich). For soluble and chromatin (oligonucleosomes) fractionations, we adapted the following protocol (Kornberg et al., 1989), with modifications (see extended experimental procedures). We analyzed protein samples by electrophoresis either on Triton Acetic acid Urea (TAU) gels to separate histone subtypes (Zweidler, 1978), or on 4-12% NuPAGE SDS-PAGE gels (Life Technologies). We tested H3.2 (van der Heijden et al., 2005) and H3.3 ((Drané et al., 2010); Abnova H00003021-M01) antibodies for specificity using wheat germ extracts (Promega, # L4380).

Supercoiling assay and MNase treatment (See extended experimental procedures for details)

We carried out supercoiling assays using High Speed Egg extracts (HSE) as described (Ray-Gallet and Almouzni, 2004), and added xHIRA antibodies (αHIRA), PBS (control) or preimmune serum (not shown) in variable volumes to monitor their blocking efficiency.

We carried out limited digestions with MNase (Nuclease S7; Micrococcal nuclease, #10107921001, Roche Diagnostics) on nuclei isolated from stage 14 embryos according to a modified protocol from (Kornberg et al., 1989).

RNA extraction, Northern Blotting and RT-qPCR

We isolated total RNA from embryos using the TRIZOL reagent (Life Technologies) or the RNeasy Mini Kit (Qiagen) to either perform a Northern blot analysis ((Brown et al., 2004), see supplemental information for probe details) or generate first-strand cDNA with random primers (Superscript III Reverse Transcriptase Kit - Life Technologies). We used cDNA to carry out RT-qPCRs with either the 7500HT Fast Real Time PCR System (Applied Biosystems) or the Light Cycler System (Roche Diagnostics). We used the SYBR Green PCR Master Mix (Applied Biosystems) and primer sequences are listed in Table S2. For each experiment, biological and technical triplicates enabled statistical analysis using a Student's t test.

COMPETING INTERESTS

The authors declare that there is no conflict of interest.

ACKNOWLEDGMENTS

We are grateful to Drs D. Ray-Gallet, A-H. Monsoro-Burq, Z. Gurard-Levin, A. Van den Berg and L. Attardi for critical reading and to members of UMR218 for helpful discussions. We thank Drs A-H. Monsoro-Burq and J. Smith for plasmids, and Dr M. Umbhauer for assistance with the animal cap assay. We thank P. de Boer for the H3.1/H3.2 antibody. G. Almouzni's team is supported by la Ligue Nationale contre le Cancer (Equipe labellisée Ligue 2010), the European Commission Network of Excellence EpiGeneSys (HEALTH-F4-2010-257082), an ERC Advanced Grant 2009-AdG_20090506 "Eccentric" and Canceropole INCa "GepiG", and E. Szenker recipient of support from the Ministère de l'Enseignement Supérieur et de la Recherche / University Pierre et Marie Curie (UPMC), Paris, France and FRM.

REFERENCES

Ahmad, K., and Henikoff, S. (2002a). Histone H3 variants specify modes of chromatin assembly. Proc Natl Acad Sci U S A *99 Suppl 4*, 16477-16484.

Ahmad, K., and Henikoff, S. (2002b). The histone variant H3.3 marks active chromatin by replication-independent nucleosome assembly. Mol Cell *9*, 1191-1200.

Almouzni, G., Khochbin, S., Dimitrov, S., and Wolffe, A.P. (1994). Histone acetylation influences both gene expression and development of Xenopus laevis. Dev Biol *165*, 654-669.

Baldessari, D., Shin, Y., Krebs, O., Konig, R., Koide, T., Vinayagam, A., Fenger, U., Mochii, M., Terasaka, C., Kitayama, A.*, et al.* (2005). Global gene expression profiling and cluster analysis in Xenopus laevis. Mech Dev *122*, 441-475.

Banaszynski, L.A., Allis, C.D., and Lewis, P.W. (2010). Histone variants in metazoan development. Dev Cell *19*, 662-674.

Boyarchuk, E., Montes de Oca, R., and Almouzni, G. (2011). Cell cycle dynamics of histone variants at the centromere, a model for chromosomal landmarks. Curr Opin Cell Biol.

Braunschweig, U., Hogan, G.J., Pagie, L., and van Steensel, B. (2009). Histone H1 binding is inhibited by histone variant H3.3. EMBO J *28*, 3635-3645.

Brown, T., Mackey, K., and Du, T. (2004). Analysis of RNA by northern and slot blot hybridization. Curr Protoc Mol Biol *Chapter 4*, Unit 4 9.

Chow, C.M., Georgiou, A., Szutorisz, H., Maia e Silva, A., Pombo, A., Barahona, I., Dargelos, E., Canzonetta, C., and Dillon, N. (2005). Variant histone H3.3 marks promoters of transcriptionally active genes during mammalian cell division. EMBO Rep *6*, 354-360.

Conlon, F.L., Sedgwick, S.G., Weston, K.M., and Smith, J.C. (1996). Inhibition of Xbra transcription activation causes defects in mesodermal patterning and reveals autoregulation of Xbra in dorsal mesoderm. Development *122*, 2427-2435.

Couldrey, C., Carlton, M., Nolan, P., Colledge, X., and Evans, M. (1999). A retroviral gene trap insertion into the histone 3.3A gene causes partial neonatal lethality, stunded growth, neuromuscular deficits and male sub-fertility in transgenic mice. Oxford University Press *8*, 2489-2495.

Cui, B., Liu, Y., and Gorovsky, M.A. (2006). Deposition and function of histone H3 variants in Tetrahymena thermophila. Mol Cell Biol *26*, 7719-7730.

De Koning, L., Corpet, A., Haber, J.E., and Almouzni, G. (2007). Histone chaperones: an escort network regulating histone traffic. Nat Struct Mol Biol *14*, 997-1007.

Dimitrov, S., Almouzni, G., Dasso, M., and Wolffe, A.P. (1993). Chromatin transitions during early Xenopus embryogenesis: changes in histone H4 acetylation and in linker histone type. Dev Biol *160*, 214-227.

Drané, P., Ouararhni, K., Depaux, A., Shuaib, M., and Hamiche, A. (2010). The death-associated protein DAXX is a novel histone chaperone involved in the replication-independent deposition of H3.3. Genes Dev *24*, 1253-1265.

Elsaesser, S.J., Goldberg, A.D., and Allis, C.D. (2010). New functions for an old variant: no substitute for histone H3.3. Curr Opin Genet Dev *20*, 110-117.

Fisher, M.E., Isaacs, H.V., and Pownall, M.E. (2002). eFGF is required for activation of XmyoD expression in the myogenic cell lineage of Xenopus laevis. Development *129*, 1307-1315.

Goldberg, A.D., Banaszynski, L.A., Noh, K.M., Lewis, P.W., Elsaesser, S.J., Stadler, S., Dewell, S., Law, M., Guo, X., Li, X.*, et al.* (2010). Distinct factors control histone variant H3.3 localization at specific genomic regions. Cell *140*, 678-691.

Green, J. (1999). The animal cap assay. Methods Mol Biol *127*, 1-13.

Hake, S.B., Garcia, B.A., Duncan, E.M., Kauer, M., Dellaire, G., Shabanowitz, J., Bazett-Jones, D.P., Allis, C.D., and Hunt, D.F. (2006). Expression patterns and post-translational modifications associated with mammalian histone H3 variants. J Biol Chem *281*, 559-568.
Heasman, J. (2006). Patterning the early Xenopus embryo. Development *133*, 1205-1217.
Hensey, C., and Gautier, J. (1997). A developmental timer that regulates apoptosis at the onset of gastrulation. Mech Dev *69*, 183-195.
Herrmann, B.G., and Kispert, A. (1994). The T genes in embryogenesis. Trends Genet *10*, 280-286.
Hodl, M., and Basler, K. (2009). Transcription in the absence of histone H3.3. Curr Biol *19*, 1221-1226.
Isaacs, H.V., Pownall, M.E., and Slack, J.M. (1994). eFGF regulates Xbra expression during Xenopus gastrulation. EMBO J *13*, 4469-4481.
Jenuwein, T., and Allis, C.D. (2001). Translating the histone code. Science *293*, 1074-1080.
Jin, C., and Felsenfeld, G. (2006). Distribution of histone H3.3 in hematopoietic cell lineages. Proc Natl Acad Sci U S A *103*, 574-579.
Jin, C., and Felsenfeld, G. (2007). Nucleosome stability mediated by histone variants H3.3 and H2A.Z. Genes Dev *21*, 1519-1529.
Jin, C., Zang, C., Wei, G., Cui, K., Peng, W., Zhao, K., and Felsenfeld, G. (2009). H3.3/H2A.Z double variant-containing nucleosomes mark 'nucleosome-free regions' of active promoters and other regulatory regions. Nat Genet *41*, 941-945.
Katagiri, C., and Ohsumi, K. (1994). Remodeling of sperm chromatin induced in egg extracts of amphibians. Int J Dev Biol *38*, 209-216.
Konev, A.Y., Tribus, M., Park, S.Y., Podhraski, V., Lim, C.Y., Emelyanov, A.V., Vershilova, E., Pirrotta, V., Kadonaga, J.T., Lusser, A.*, et al.* (2007). CHD1 motor protein is required for deposition of histone variant H3.3 into chromatin in vivo. Science *317*, 1087-1090.
Kornberg, R.D., LaPointe, J.W., and Lorch, Y. (1989). Preparation of nucleosomes and chromatin. Methods Enzymol *170*, 3-14.
Laskey, R.A., Honda, B.M., Mills, A.D., and Finch, J.T. (1978). Nucleosomes are assembled by an acidic protein which binds histones and transfers them to DNA. Nature *275*, 416-420.
Latinkic, B.V., Umbhauer, M., Neal, K.A., Lerchner, W., Smith, J.C., and Cunliffe, V. (1997). The Xenopus Brachyury promoter is activated by FGF and low concentrations of activin and suppressed by high concentrations of activin and by paired-type homeodomain proteins. Genes Dev *11*, 3265-3276.
Lerchner, W., Latinkic, B.V., Remacle, J.E., Huylebroeck, D., and Smith, J.C. (2000). Region-specific activation of the Xenopus brachyury promoter involves active repression in ectoderm and endoderm: a study using transgenic frog embryos. Development *127*, 2729-2739.
Lewis, P.W., Elsaesser, S.J., Noh, K.M., Stadler, S.C., and Allis, C.D. (2010). Daxx is an H3.3-specific histone chaperone and cooperates with ATRX in replication-independent chromatin assembly at telomeres. Proc Natl Acad Sci U S A *107*, 14075-14080.
Loppin, B., Bonnefoy, E., Anselme, C., Laurencon, A., Karr, T.L., and Couble, P. (2005). The histone H3.3 chaperone HIRA is essential for chromatin assembly in the male pronucleus. Nature *437*, 1386-1390.
Loyola, A., and Almouzni, G. (2007). Marking histone H3 variants: how, when and why? Trends Biochem Sci *32*, 425-433.

Loyola, A., Bonaldi, T., Roche, D., Imhof, A., and Almouzni, G. (2006). PTMs on H3 variants before chromatin assembly potentiate their final epigenetic state. Mol Cell *24*, 309-316.
McKittrick, E., Gafken, P.R., Ahmad, K., and Henikoff, S. (2004). Histone H3.3 is enriched in covalent modifications associated with active chromatin. Proc Natl Acad Sci U S A *101*, 1525-1530.
Mito, Y., Henikoff, J.G., and Henikoff, S. (2005). Genome-scale profiling of histone H3.3 replacement patterns. Nat Genet *37*, 1090-1097.
Newport, J., and Kirschner, M. (1982). A major developmental transition in early Xenopus embryos: I. characterization and timing of cellular changes at the midblastula stage. Cell *30*, 675-686.
Ng, R.K., and Gurdon, J.B. (2008). Epigenetic memory of an active gene state depends on histone H3.3 incorporation into chromatin in the absence of transcription. Nat Cell Biol *10*, 102-109.
Nieuwkoop, P.D., and Faber, J. (1967). Normal Table of Xenopus laevis. Amsterdam: Daudin.
Orsi, G.A., Couble, P., and Loppin, B. (2009). Epigenetic and replacement roles of histone variant H3.3 in reproduction and development. Int J Dev Biol *53*, 231-243.
Probst, A.V., Dunleavy, E., and Almouzni, G. (2009). Epigenetic inheritance during the cell cycle. Nat Rev Mol Cell Biol *10*, 192-206.
Quivy, J.P., Grandi, P., and Almouzni, G. (2001). Dimerization of the largest subunit of chromatin assembly factor 1: importance in vitro and during Xenopus early development. EMBO J *20*, 2015-2027.
Ray-Gallet, D., and Almouzni, G. (2004). DNA synthesis-dependent and -independent chromatin assembly pathways in Xenopus egg extracts. Methods Enzymol *375*, 117-131.
Ray-Gallet, D., Quivy, J.P., Scamps, C., Martini, E.M., Lipinski, M., and Almouzni, G. (2002). HIRA is critical for a nucleosome assembly pathway independent of DNA synthesis. Mol Cell *9*, 1091-1100.
Ray-Gallet, D., Woolfe, A., Vassias, I., Pellentz, C., Lacoste, N., Puri, A., Schultz, D.C., Pchelintsev, N.A., Adams, P.D., Jansen, L.E.*, et al.* (2011). Dynamics of histone H3 deposition in vivo reveal a nucleosome gap-filling mechanism for H3.3 to maintain chromatin integrity. Mol Cell *44*, 928-941.
Ridgway, P., Brown, K.D., Rangasamy, D., Svensson, U., and Tremethick, D.J. (2004). Unique residues on the H2A.Z containing nucleosome surface are important for Xenopus laevis development. J Biol Chem *279*, 43815-43820.
Roche, D., Almouzni, G., and Quivy, J.P. (2006). Chromatin assembly of DNA templates microinjected into Xenopus oocytes. Methods Mol Biol *322*, 139-147.
Sakai, A., Schwartz, B.E., Goldstein, S., and Ahmad, K. (2009). Transcriptional and Developmental Functions of the H3.3 Histone Variant in Drosophila. Curr Biol *19*, 1816-1820.
Santenard, A., Ziegler-Birling, C., Koch, M., Tora, L., Bannister, A.J., and Torres-Padilla, M.E. (2010). Heterochromatin formation in the mouse embryo requires critical residues of the histone variant H3.3. Nat Cell Biol *12*, 853–862.
Sarma, K., and Reinberg, D. (2005). Histone variants meet their match. Nat Rev Mol Cell Biol *6*, 139-149.
Schwartz, B.E., and Ahmad, K. (2005). Transcriptional activation triggers deposition and removal of the histone variant H3.3. Genes Dev *19*, 804-814.
Schwartzentruber, J., Korshunov, A., Liu, X.Y., Jones, D.T., Pfaff, E., Jacob, K., Sturm, D., Fontebasso, A.M., Quang, D.A., Tonjes, M.*, et al.* (2012). Driver mutations in histone H3.3 and chromatin remodelling genes in paediatric glioblastoma. Nature *482*, 226-231.

Showell, C., Binder, O., and Conlon, F.L. (2004). T-box genes in early embryogenesis. Dev Dyn *229*, 201-218.
Sive, H.L., Grainger, R.M., and Hardland, R.M. (2000). Early development of Xenopus laevis. A laboratory manual. (Cold Spring Harbor Laboratory Press).
Smith, S., and Stillman, B. (1989). Purification and characterization of CAF-I, a human cell factor required for chromatin assembly during DNA replication in vitro. Cell *58*, 15-25.
Steinbach, O.C., Wolffe, A.P., and Rupp, R.A. (1997). Somatic linker histones cause loss of mesodermal competence in Xenopus. Nature *389*, 395-399.
Suzuki, A., Nagai, T., Nishimatsu, S., Sugino, H., Eto, Y., Shibai, H., Murakami, K., and Ueno, N. (1994). Autoinduction of activin genes in early Xenopus embryos. Biochem J *298 (Pt 2)*, 275-280.
Szenker, E., Ray-Gallet, D., and Almouzni, G. (2011). The double face of the histone variant H3.3. Cell Res.
Tachiwana, H., Osakabe, A., Shiga, T., Miya, Y., Kimura, H., Kagawa, W., and Kurumizaka, H. (2011). Structures of human nucleosomes containing major histone H3 variants. Acta Crystallogr D Biol Crystallogr *67*, 578-583.
Tagami, H., Ray-Gallet, D., Almouzni, G., and Nakatani, Y. (2004). Histone H3.1 and H3.3 complexes mediate nucleosome assembly pathways dependent or independent of DNA synthesis. Cell *116*, 51-61.
Torres-Padilla, M.E., Bannister, A.J., Hurd, P.J., Kouzarides, T., and Zernicka-Goetz, M. (2006). Dynamic distribution of the replacement histone variant H3.3 in the mouse oocyte and preimplantation embryos. Int J Dev Biol *50*, 455-461.
Turner, B.M. (2002). Cellular memory and the histone code. Cell *111*, 285-291.
van der Heijden, G.W., Dieker, J.W., Derijck, A.A., Muller, S., Berden, J.H., Braat, D.D., van der Vlag, J., and de Boer, P. (2005). Asymmetry in histone H3 variants and lysine methylation between paternal and maternal chromatin of the early mouse zygote. Mech Dev *122*, 1008-1022.
Vermaak, D., Steinbach, O.C., Dimitrov, S., Rupp, R.A., and Wolffe, A.P. (1998). The globular domain of histone H1 is sufficient to direct specific gene repression in early Xenopus embryos. Curr Biol *8*, 533-536.
Verschueren, K., Remacle, J.E., Collart, C., Kraft, H., Baker, B.S., Tylzanowski, P., Nelles, L., Wuytens, G., Su, M.T., Bodmer, R.*, et al.* (1999). SIP1, a novel zinc finger/homeodomain repressor, interacts with Smad proteins and binds to 5'-CACCT sequences in candidate target genes. J Biol Chem *274*, 20489-20498.
Watabe, T., and Miyazono, K. (2009). Roles of TGF-beta family signaling in stem cell renewal and differentiation. Cell Res *19*, 103-115.
Waterborg, J.H. (1990). Sequence analysis of acetylation and methylation in two histone H3 variants of alfalfa. J Biol Chem *265*, 17157-17161.
Wu, G., Broniscer, A., McEachron, T.A., Lu, C., Paugh, B.S., Becksfort, J., Qu, C., Ding, L., Huether, R., Parker, M.*, et al.* (2012). Somatic histone H3 alterations in pediatric diffuse intrinsic pontine gliomas and non-brainstem glioblastomas. Nat Genet *44*, 251-253.
Wysocka, J., Swigut, T., Milne, T.A., Dou, Y., Zhang, X., Burlingame, A.L., Roeder, R.G., Brivanlou, A.H., and Allis, C.D. (2005). WDR5 associates with histone H3 methylated at K4 and is essential for H3 K4 methylation and vertebrate development. Cell *121*, 859-872.
Yang, J.H., Song, Y., Seol, J.H., Park, J.Y., Yang, Y.J., Han, J.W., Youn, H.D., and Cho, E.J. (2011). Myogenic transcriptional activation of MyoD mediated by replication-independent histone deposition. Proc Natl Acad Sci U S A *108*, 85-90.

Zweidler, A. (1978). Resolution of histones by polyacrylamide gel electrophoresis in presence of nonionic detergents. Methods Cell Biol *17*, 223-233.

FIGURE LEGENDS

Figure 1: Importance of H3.2 and H3.3 during early development. **(A) Specificity of H3.3 and H3 morpholinos.** (Left) The scheme shows injections of indicated morpholinos (MO) in fertilized eggs (13.8ng). After incubation to reach stage 12 in controls, 80 embryos served to prepare soluble fractions for Western blot analysis. (Right) Results used a 2-fold dilution series (gradient bar) with the highest quantity being equivalent to 3 embryos, and detection with indicated antibodies (see also Figure S2A). Anti-βactin and memcode staining served as loading controls. **(B) H3.3 and H3 downregulation leads to distinct phenotypes.** The scheme shows injections of indicated MO (4.6ng) in one cell of two-cell stage embryos. We kept embryos at 18°C and acquired images at the indicated stages (using control embryos as a reference). White arrows point to the gastrulation defects in H3.3 morphants. In the bottom panel, we show a broader coverage of the gastrulation time period (stages 11 to 13) with 8 distinct time points (see also Movie S1). Scale bar: 1mm. See also Figures S1, S2 and S3.

Figure 2: Additional H3.2 cannot bypass the need for H3.3. (A) HA tagged-H3.2 and -H3.3 proteins can be incorporated into chromatin. (Left) The scheme shows injections of indicated mRNA (500pg) in one cell of 2-cell stage embryos. After incubation to reach stage 11 in controls, 50 embryos served to prepare chromatin for Western blot analysis. (Right) Results used a 2-fold dilution series (gradient bar) with the highest quantity being equivalent to 2 embryos, and detection with indicated antibodies. Anti-H4 served as a loading control. **(B) Expression of histone chaperones in H3.3-deficient embryos.** (Left) The scheme shows injections of H3.3 MO (23ng) in fertilized eggs. After incubation to reach stage 14 in controls, 40

non-injected (-) and 40 injected (MO H3.3) embryos served to prepare soluble fractions for Western blot analysis. (Right) Results used a 2-fold dilution series (gradient bar) with the highest quantity being equivalent to 3 embryos, and detection with indicated antibodies. Anti-βactin served as a loading control. We note that H3.3 downregulation leads to overexpression of HIRA in soluble fractions. **(C) H3.3 but not H3.2 mRNAs can rescue the H3.3-deficient phenotype.** The scheme shows injections of indicated MO (46ng for CTL and 4.6ng for H3.3) in one cell of two-cell stage embryos followed by a second injection with indicated mRNAs (2ng). After incubation to reach stage 25 in control embryos, 3 embryos served for image acquisition (top panel) and followed by total protein extraction for Western blot analysis (bottom panel). **Top panel:** We scored the viability for 30 embryos (percentage is shown). Scale bar: 1mm. **Bottom panel:** We loaded the equivalent of 0.5 and 0.25 embryo (gradient bar) and revealed with indicated antibodies. Anti-tubulin served as a loading control. See also Figures S2 and S3.

Figure 3: The early mesodermal marker Xbra is misregulated in the absence of H3.3. (A) Xbra expression pattern defects in H3.3 morpholino injected embryos. The scheme shows injections of indicated MO (69ng of CTL, 4.6ng of either H3.3 or mutH3.3 MO) in one cell of 4-cell stage embryos. After incubation to reach the indicated stages in controls, we fixed embryos and performed whole mount *in situ* hybridization with an Xbra probe. White arrows indicate the injected part and arrowheads the non-injected part of H3.3 morphants. Scale bar: 1mm. **(B) Expression level of developmental genes.** The scheme shows injections of indicated MO (9.2ng) in fertilized eggs. After incubation to reach stage 11 (gastrula) in controls, embryos served to prepare total RNA extracts and analysis by RT-qPCR of indicated genes (See also Figure S4A). We represent the expression of a series of

genes in H3.3 morphants compared to controls. Red boxes show genes that are significantly downregulated and gray boxes genes whose expression is not significantly affected. Statistical test from 8 independent experiments performed in duplicates: Paired Student's t test, p-value <0.05. See also Figure S4.

Figure 4: H3.3 downregulation does not affect animal caps elongation upon mesoderm induction but leads to cell death. (A) Animal Cap assay using MO H3.3 treated embryos. The scheme shows injections in both cells of two-cell stage embryos with indicated MO [2.5ng/cell (=5ng) or 4.6ng/cell (=9.2ng)] or with Xbra-EnR mRNA [250pg/cell (=500pg)], a dominant negative form of Xbra as a negative control. After incubation to reach stage 8 in controls, we dissected animal caps in each case for incubation with or without Activin (5ng/ml) for 1.5h, and cultured them until sibling embryos reached the neurula stage. For the low MO dose (5ng), we show an inset of one representative animal cap elongation at the same magnification scale as the other panels. Scale bar: 1mm. **(B) Analysis of H3.3 morpholino injected embryos throughout development.** The scheme shows injections of indicated MO (4.6ng) in one cell of 2-cell stage embryos. We followed development at 18°C of one Control (white box) and five H3.3 morphants with acquisition from the vegetative pole (see also Movie S2). Here are three time points: 64 cells, gastrula, and neurula stage. White arrows indicate the apoptotic cells observed at the end of the gastrulation. Scale bar: 1mm. **(C) TUNEL assay of MO H3.3 treated embryos.** We injected the indicated MO (4.6ng) in one cell of two-cell stage embryos and performed a TUNEL assay when controls embryos reached the neurula and tailbud stages. White arrows indicate the TUNEL positive cells in the injected side of H3.3 morphants. The majority of white apoptotic cells comes off the embryos at the beginning of the experimental procedure that involves dechorionization. Scale bar:

1mm. See also Figure S5.

Figure 5: HIRA downregulation resembles the H3.3 phenotype. (A) Specificity of HIRA morpholinos. (Left) The scheme shows injections of HIRA MO (92ng) in fertilized eggs. After incubation to reach stage 11 in controls, 40 non-injected (-) and 40 injected (MO HIRA) embryos served to prepare soluble extracts for Western blot analysis. (Right) Results used a 2-fold dilution series (gradient bar) with the highest quantity being equivalent to 3 embryos, and detection with a HIRA antibody. Anti-βactin and memcode staining served as loading controls. **(B) Downregulation of HIRA but not WDR5 leads to gastrulation defects.** We injected the indicated MO (46ng) in one cell of two-cell stage embryos. We acquired images when controls were at the indicated stages. White arrows indicate the gastrulation defects observed in HIRA morphants. In the bottom panel, we show a broader coverage of the gastrulation time period (stages 11 to 13) with 8 distinct time points (see also Movie S1). Scale bar: 1mm. **(C) Xbra mRNA *in situ* hybridization in HIRA- and WDR5-defcient embryos.** We injected the indicated MO (69ng for CTL or WDR5, 46ng for either HIRA or mutHIRA) in one cell of 4-cell stage embryos. After incubation to reach the indicated stages in controls, we fixed injected embryos and performed whole mount *in situ* hybridization with an Xbra probe. White arrows indicate the injected part and arrowheads the non-injected part of HIRA morphant embryos. Scale bar: 1mm. See also Figures S3 and S5.

Figure 6: HIRA is critical for H3.3 assembly during early development. (A) Nucleosome assembly independent of DNA synthesis requires HIRA *in vitro*. The scheme shows a nucleosome assembly assay independently of DNA synthesis using *Xenopus* High Speed Egg extracts (HSE). We incubated circular DNA plasmids

with HSE (5μL) during the indicated times together with antibodies targeting xHIRA (αHIRA), PBS (CTL) or preimmune serum (not shown). After deproteinization, we analyzed plasmid DNA supercoiling by electrophoresis on agarose gel stained with ethidium bromide. Input DNA run in parallel (first lane on the left, 0 minute) and migration positions of DNA plasmid form I (supercoiled), form II (nicked circular), form Ir (closed circular) are indicated. **(B) HIRA downregulation affects the level of H3.3 in the chromatin.** The scheme shows injections of indicated MO (18.4ng for H3.3 and 138ng for HIRA) in fertilized eggs. After incubation to reach stage 14 in controls (-), 40 embryos in each case served to prepare soluble and chromatin fractions for Western blot analysis. Results used a 2-fold dilution series (gradient bar) with the highest quantity being equivalent to 3 embryos, and detection with antibodies. Anti-βactin and memcode staining served as loading controls. We note that H3.3 downregulation leads to overexpression of HIRA in soluble fractions. **(C) MNase digestion profile of H3.3 and HIRA MO injected embryos.** We injected 18.4ng of H3.3 and 138ng of HIRA MO in fertilized eggs. After incubation to reach stage 14 in non-injected controls (CTL1 and 2), 40 embryos in each case served to prepare nuclei that we subjected to MNase digestion for increasing indicated incubation times. For each time point, we purified the resulting DNA fragments from the equivalent of 1.5 embryos to be analyzed by electrophoresis on agarose gel stained with ethidium bromide. Densitometric profiles of the 1 min digestion products are shown on the right.

Figure 1

Click here to download high resolution image

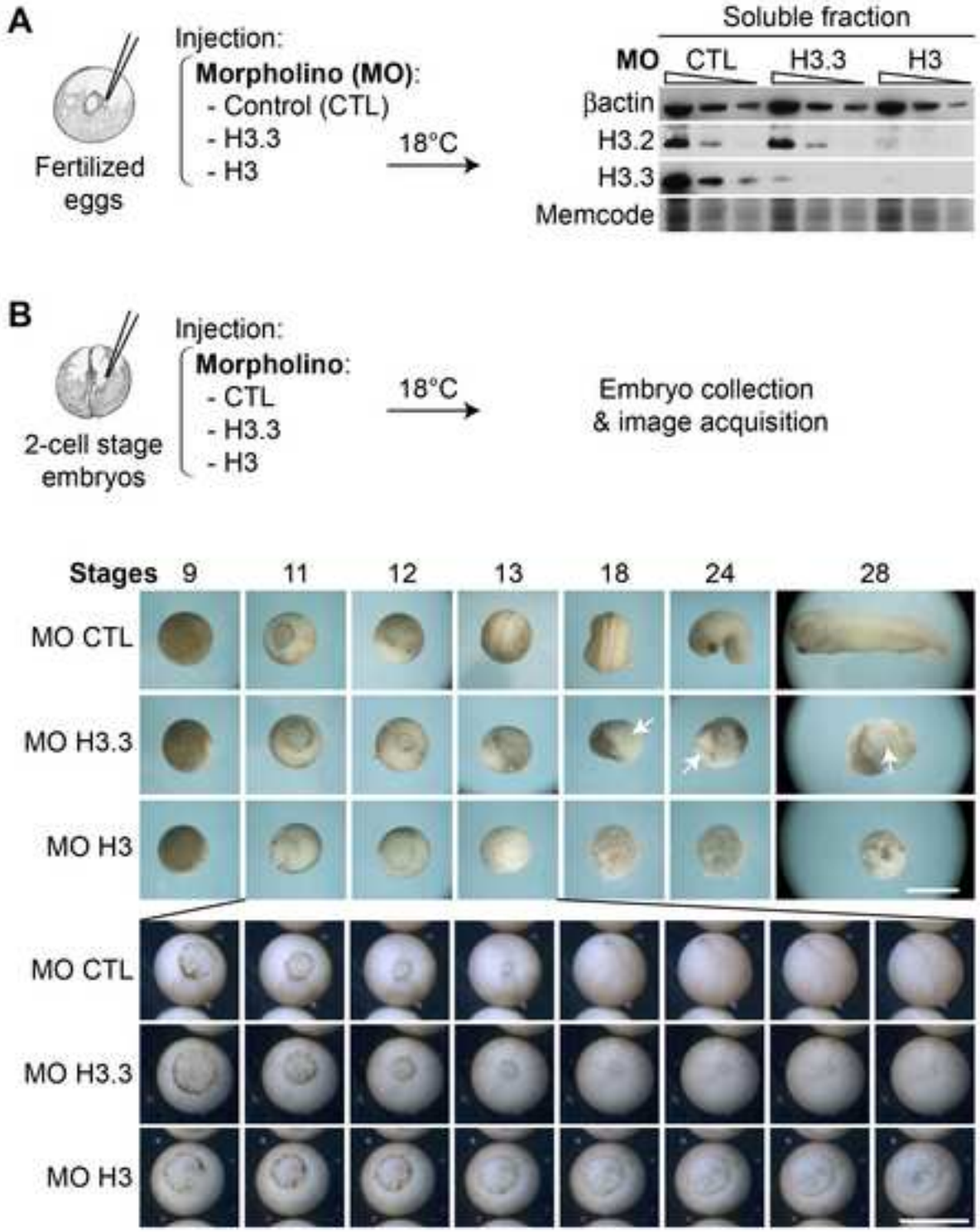

Figure 1

Figure 2

Click here to download high resolution image

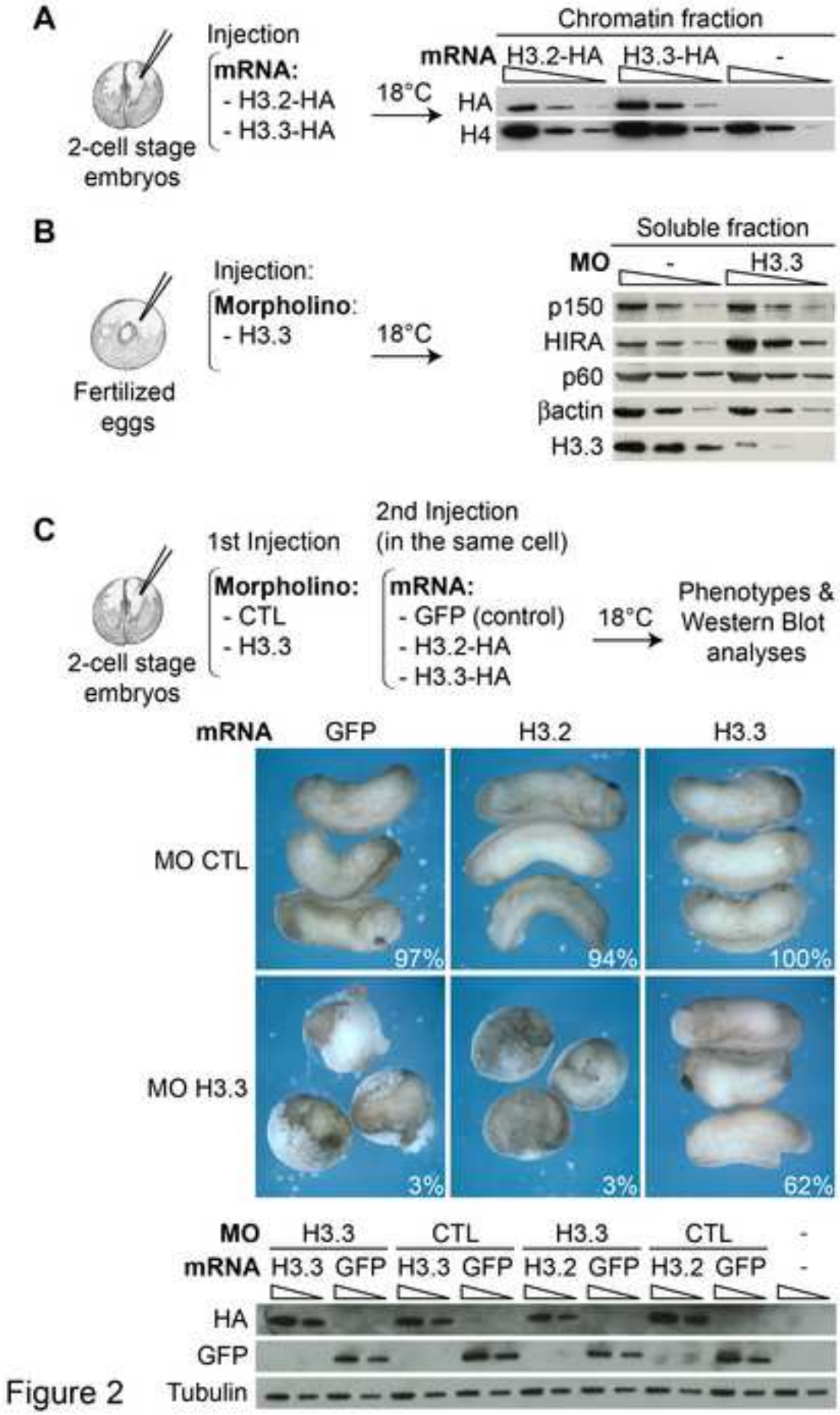

Figure 2

Figure 3

Click here to download high resolution image

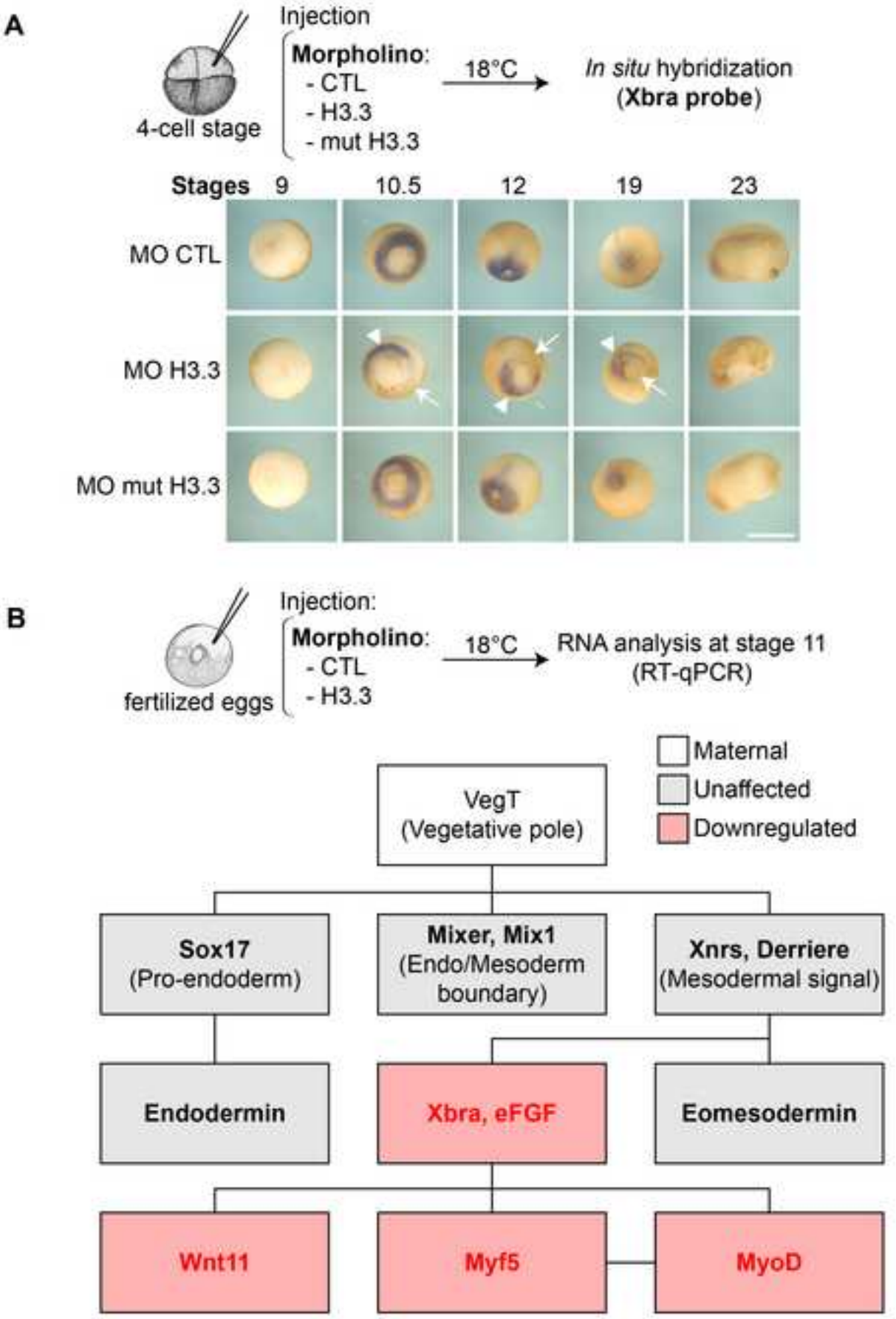

Figure 3

Figure 4

Click here to download high resolution image

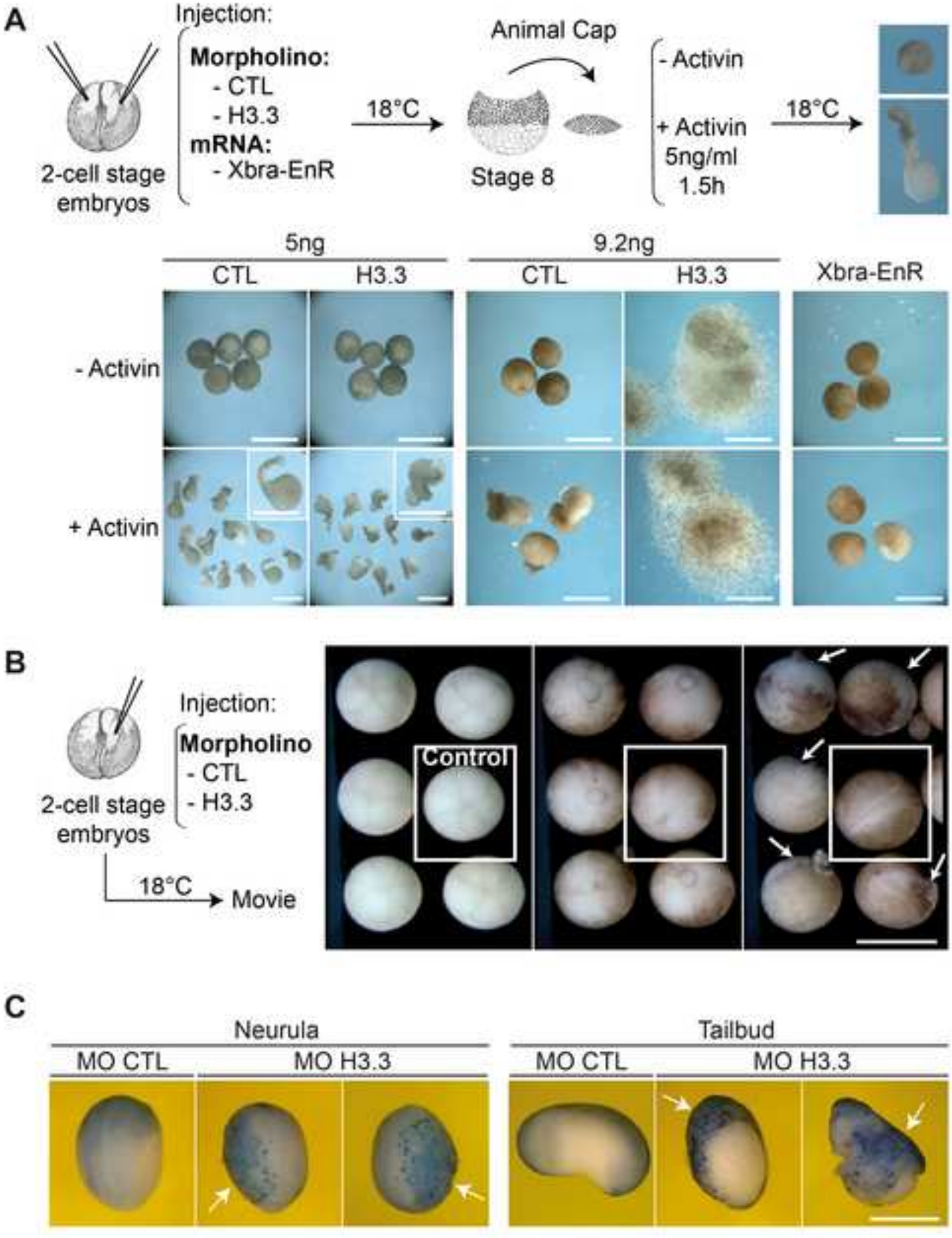

Figure 4

Figure 5

Click here to download high resolution image

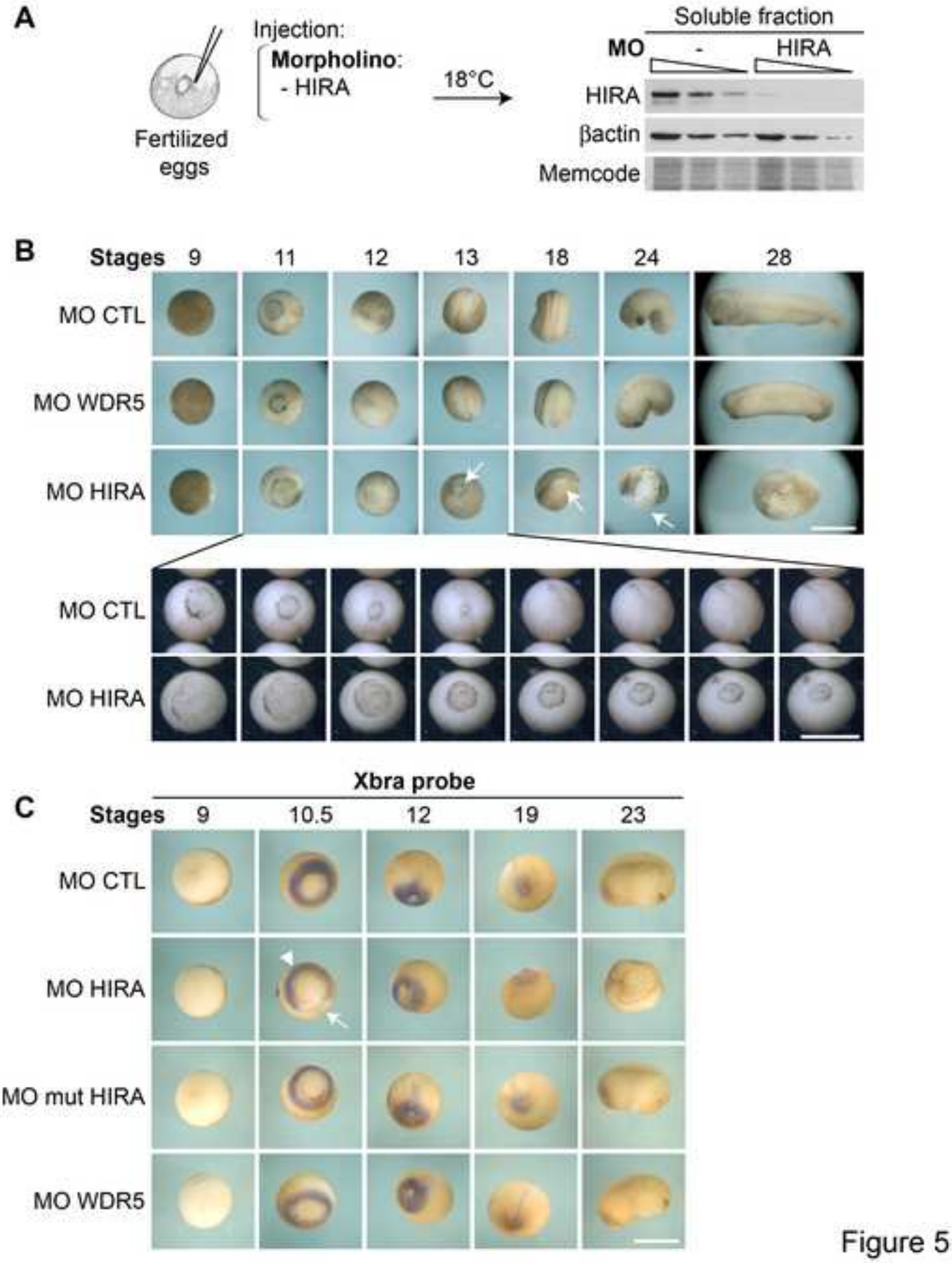

Figure 5

Figure 6

Click here to download high resolution image

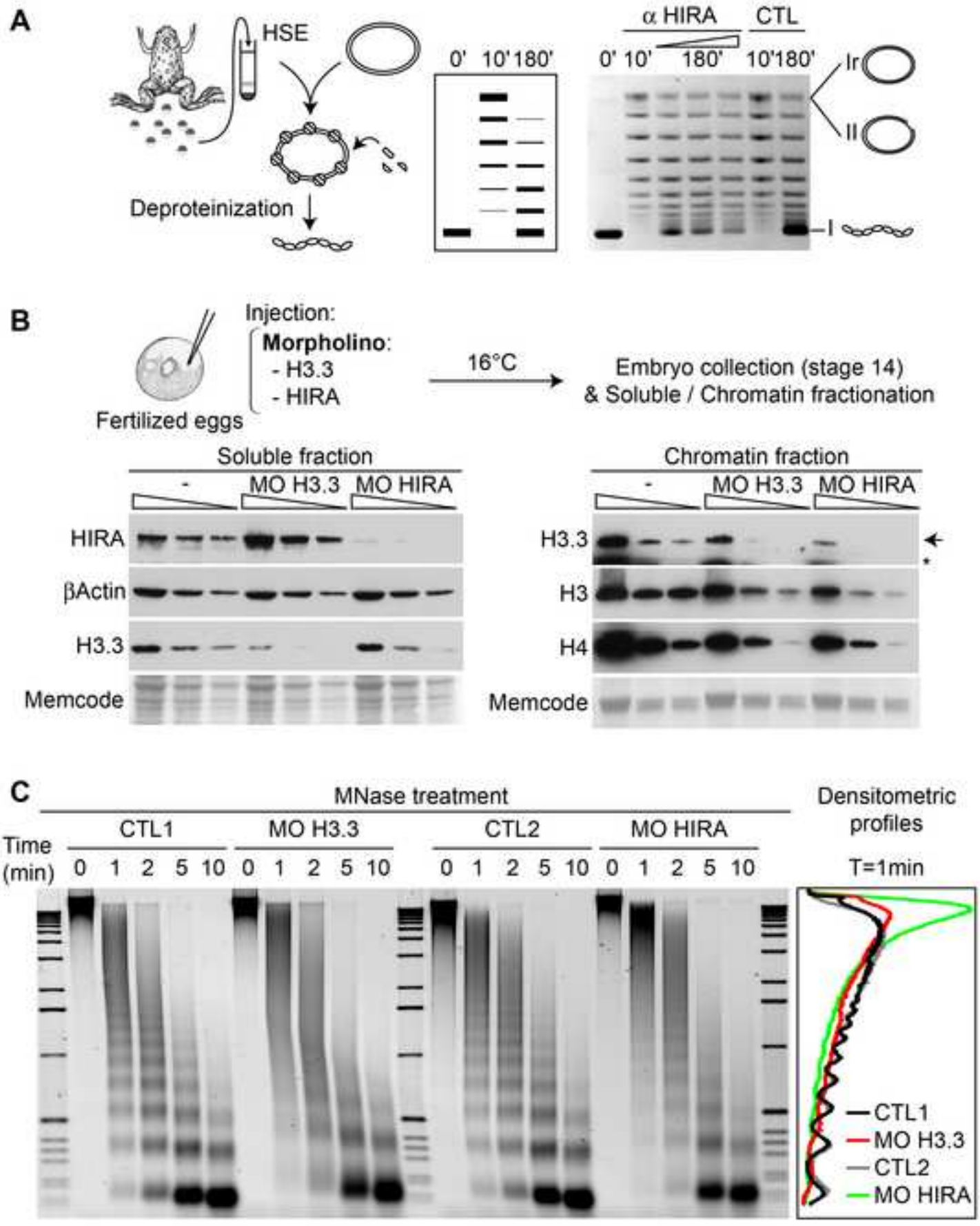

Figure 6

EXTENDED EXPERIMENTAL PROCEDURES

Xenopus laevis experimentation

We used *Xenopus laevis* adults from Centre Ressource Biologie "Xenope" for experiments approved by the Comité d'Ethique en matière d'Expérimentation Animale Ile de France Paris 1.

Northern blot and in situ hybridization probes

We used 500bp of the 3'UTR of the H3.2a (NCBI # X03104) or the H3.3b (BC042290) gene cloned into pCR4TOPO (Life Technologies) to produce specific *in situ* probes. We obtained a total H3 probe by mixing H3.2b (BC084311) and H3.3b cDNAs probes**.** We used the same sequences to produce Northern blot probes. We obtained a HIRA *in situ* probe from a pCR4TOPO-xHIRA construct (BC078007). We also used the following plasmids: psp73-Xbra (provided by Pr. J. Smith, MRC, London), and pBluescriptKS-MyoD (BC041190), pBluescriptSK-Sip1 (AB038353), pBluescriptSK-Sox17a (BC106403) (plasmids provided by Pr. A-H. Monsoro-Burq, Institut Curie, France).

Soluble and Chromatin fractionation

To prepare soluble and chromatin (oligonucleosomes) fractions from embryos, we adapted the method from (Kornberg et al., 1989). Briefly, we homogenized 40 embryos in 200μL of the following Lysis Buffer [Tris-HCl pH=7.5 10mM, NaCl 200mM, $MgCl_2$ 5mM, NP40 0.5%, complete EDTA-free 1X (Roche Diagnostics, # 11873580001)]. After a centrifugation at 1000g for 2 minutes at 4°C, we further ultracentrifuged the supernatant at 160,000g for 1 hour at 4°C to obtain a clear soluble fraction. For chromatin fractions, we homogenized 40 embryos with a Lysis Buffer containing only 10mM NaCl. After a centrifugation at 1000g for 2min and

several washes with the same buffer, we washed the pellet in the Buffer A [Tris-HCl pH=7.5, NaCl 15mM, KCl 60mM, sucrose 0.34M, DTT 1mM, complete EDTA-free 1X] and then resuspended it in 400 μL of this buffer. After addition of $CaCl_2$ (2mM final) and RNase A (Roche Diagnostics, #10109142001) treatment (75μg/ml final, 5min at 37°C), we exposed nuclei to micrococcal nuclease digestion (MNase, Roche Diagnostics, #1010792100) with 11.25U/mL final during 10min (or as indicated) at 37°C. We stopped the digestion by adding EDTA (50mM final) and recovered the solubilized chromatin fraction after a centrifugation at 1000g for 2min.

Detailed Supercoiling assay and MNase treatment

We carried out supercoiling assays using High Speed Egg extracts (HSE) as described (Ray-Gallet and Almouzni, 2004), and added xHIRA antibodies (αHIRA), PBS (control) or preimmune serum (not shown) in variable volumes to monitor their blocking efficiency. After incubation during the indicated time at 23°C, we stopped the reaction by adding 25μL of the following mix [30mM EDTA, 0.7% SDS]. We recovered DNA after RNase (Roche Diagnostics, #10109142001, 0.1mg/mL final, 30min at 37°C) and Proteinase K treatment (Roche Diagnostics, #03115879001, 0.2mg/mL final, 30min at 37°C) followed by phenol/chloroform extraction and ethanol precipitation. Purified plasmid DNA was subjected to agarose gel electrophoresis (1.2% agarose in 1XTAE buffer, migration at 2V/cm for 16 hours at 4°C) to resolve the topological forms. We used ethidium bromide staining for visualization with a Typhoon FLA 9000 (GE Healthcare-Life Sciences).

For MNase experiments shown in Figure 6C, we recovered DNA after Proteinase K treatment followed by phenol/chloroform extraction and ethanol precipitation. Purified

DNA was subjected to agarose gel electrophoresis (1.5% agarose in 1XTAE buffer, migration at 4V/cm for 4 hours) to analyze the extent of digestion. We used ethidium bromide staining for visualization with a Typhoon FLA 9000 (GE Healthcare-Life Sciences).

We also prepared soluble fractions using the High Speed Egg (HSE) extract protocol (Ray-Gallet and Almouzni, 2004) to be analyzed by electrophoresis in a Triton Acetic acid Urea (TAU) gel and separate histone subtypes (Zweidler, 1978).

mRNAs preparation

We *in vitro* transcribed capped mRNA from GFP, xH3.2-HA and hH3.3-HA cloned into the pβRN3P vector (Zernicka-Goetz et al., 1996) using T3 RNA polymerase (Promega). The plasmid pSP64T-Xbra-EnR was kindly provided by J. Smith.

Antibodies

After gel transfer on nitrocellulose membranes (Protran) for western blotting, we used specific antibodies and revelation was performed with the Super Signal detection kit (Thermo Scientific). We used the following primary antibodies: anti- H3 (Abcam ab1791; 1:1,000 dilution), anti- H3.1/H3.2 ((van der Heijden et al., 2005); 1:1,000), anti- H3.3 (Abnova H00003021-M01; 1:40), anti- H4 (Millipore #05-858; 1:1,000), anti- HA (Roche Diagnostics Clone 3F10; 1:1,000), anti- xHIRA ((Ray-Gallet et al., 2002); 1:2,000), anti- xp150 ((Quivy et al., 2001); 1:1,000), anti- xp60 ((Ray-Gallet et al., 2007); 1:1,000), anti- GFP (SantaCruz #SC8334; 1:500), anti- βactin (Sigma-Aldrich #a5441; 1:2,000), anti- α-tubulin (Sigma-Aldrich #T9026; 1:10,000). Secondary antibodies used were HRP-conjugated affinity-purified sheep anti–mouse or donkey anti–rabbit (1:20,000; Jackson ImmunoResearch Laboratories, Inc.).

SUPPLEMENTAL FIGURE TITLES AND LEGENDS

Figure S1: H3 and H3.3 regulation during early development, Related to Figure 1. **(A) H3 and H3.3 expression levels by Northern Blot.** We extracted total RNAs from embryos at indicated developmental stages for analysis of H3.2 and H3.3 transcripts by Northern Blot. We show the signals for total H3 transcripts (H3.2+H3.3 cDNA), total RNA visualized by methylene blue (revealing the 28S and 18s rRNAs), H3.2 and H3.3 single transcripts (H3.2b+H3.3b 3'UTR) and single H3.3 transcript (H3.3b 3'UTR). **(B) Expression pattern of H3.2 and H3.3 mRNA during *Xenopus* development.** We fixed embryos at indicated stages and performed whole mount *in situ* hybridization using DIG-UTP RNA probes. We show the expression pattern of total H3 (H3.2+H3.3 cDNA), H3.2a, H3.3b and HIRA single transcripts (3'UTR). The Sox17α probe served as a reference for endoderm staining, and a sense probe was used as a negative control. We sectioned stage 9 and 11 embryos prior to the *in situ* hybridization procedure. Scale bars: 1mm, sketches adapted from (Nieuwkoop and Faber, 1967). **(C) Soluble pool of H3.2 versus H3.3 levels throughout development.** We prepared HSE extracts from eggs and embryos at indicated stages for analysis by Triton Acid Urea (TAU) gel electrophoresis. This allowed the separation of H3.2 and H3.3 variants that we revealed by Western blot with an H3 antibody. Memcode staining served as a loading control, MBT=Mid Blastula Transition, sketches adapted from (Nieuwkoop and Faber, 1967).

Figure S2: Specificity of H3.2 and H3.3 antibodies and histone chaperones phenotypes during early development, Related to Figures 1 and 2. (A) Specificity of H3.2 and H3.3 antibodies. We used wheat germ extracts to *in vitro* translate H3.2-HA and H3.3-HA mRNAs and analyzed them by Western blot using

specific antibodies as indicated. Asterisks (*) show unspecific bands also present in extracts without exogenous mRNA (-) while the arrow indicates the H3-HA band (H3.2-HA or H3.3-HA). Memcode staining served as a loading control. **(B) HIRA phenotype phenocopies H3.3 phenotype while MO p150 phenocopies the one of MO H3 injected embryos.** We injected indicated MO (13.8ng for H3 and H3.3, 138ng for CTL, p150 and HIRA MO) in one cell of two-cell stage embryos. We show the gastrulation time periode between stages 11 and 13 with 8 distinct time points (see also Figure 1, Figure 5, and Movie S1). Scale bar: 1mm.

Figure S3: Dose dependent phenotypes and chaperone expression throughout development, Related to Figures 1 and 2. (A) Dose-dependent phenotype of H3.3 and HIRA morpholinos. We injected CTL, H3.3 or HIRA MO (at the indicated doses) in one cell of two-cell stage embryos and acquired images when control embryos reached stage 28. Scale bar: 1mm. **(B) Expression of histone chaperones during early development.** Embryos at indicated stages served to prepare soluble fractions and analysis by Western blot. We used a 2-fold dilution series as indicated (gradient bar) with the highest quantity being equivalent to 3 embryos, and revealed with specific antibodies as indicated. βactin served as a loading control. Asterisk (*) shows an unspecific band, sketches are adapted from (Nieuwkoop and Faber, 1967). **(C) Control injection phenotypes.** We injected the indicated MO (4.6ng of mutH3 and mutH3.3 MO, 46ng of CTL and mutHIRA MO) in one cell of two-cell stage embryos and acquired images when control embryos reached stage 28. Scale bar: 1mm.

Figure S4: Specific effects of H3.3 MO on the transcription of mesoderm genes, Related to Figure 3. (A) RT-qPCR expression profiling of MO H3.3 treated embryos. We injected CTL or H3.3 MO (9.2ng) in fertilized eggs. After incubation at 18°C to reach stage 11 (gastrula) in controls, embryos served in each case to prepare total RNA extracts and analysis by RT-qPCR of indicated genes. We represent graphically in a $\log_2$ scale the fold changes between MO H3.3 and MO CTL embryos, first normalized to the housekeeping gene ODC. We classified genes according to their importance for the endoderm, mesoderm, neuroctoderm or epiderm regulatory networks. Red shows genes that are significantly downregulated in MO H3.3, while green indicates significantly overexpressed genes. In gray are genes whose expression is not affected (* Paired Student's t test p-value <0.05). Plotted are means and standard deviations of 8 independent experiments performed in duplicates. **(B) Spatio-temporal expression of specific markers in MO H3.3 treated embryos.** We injected the indicated MO (4.6ng) in one cell of 2-cell stage embryos and performed whole mount *in situ* hybridization with specific probes and stages as indicated. White arrows indicate the injected side and arrowheads the uninjected part of H3.3 morphant embryos. Scale bar: 1mm

Figure S5: Control injection experiments, Related to Figures 4 and 5. (A) Xbra-EnR phenotype. We injected Xbra-EnR mRNA (500pg) in one cell of two-cell stage embryos and acquired images when controls reached stage 28. Xbra-EnR injected embryos exhibit defects of the posterior mesoderm development (Conlon et al, 1999). Scale bar: 1mm. **(B) WDR5 phenotype.** We injected indicated MO (46ng) in one cell of two-cell stage embryos and acquired images when control embryos reached the tadpole stage. MO WDR5-injected tadpoles exhibit abnormal distribution

of blood cells (blood is absent from heart while forming a hemorrhage in the tail – black arrows), and failure of gut patterning (white arrows). Some tadpoles also exhibited body curvature (not shown) (Wysocka et al., 2005). Scale bar: 1mm.

SUPPLEMENTAL MOVIE TITLES AND LEGENDS

Movie S1: Development of MO H3, H3.3, p150, and HIRA treated embryos compared to controls from blastula to tailbud stage, Related to Figures 1, 5 and S2. We injected CTL (138ng), H3 (13.8ng), p150 (138ng), H3.3 (13.8ng), or HIRA (138ng) MO in one cell of two-cell stage embryos and followed development of two injected embryos in each case from the vegetal side.

Movie S2: Development of H3.3-deficient compared to a control embryo from blastula to neurula stage, Related to Figure 4. We injected CTL or H3.3 (4.6ng) in one cell of two-cell stage embryos and followed development of one Control (white boxed) and five H3.3 morphants. Note the apoptotic cells observed in the end of the gastrulation of H3.3 morphants. View from the vegetative side.

SUPPLEMENTAL TABLES

Table S1: List of morpholinos, related to Experimental procedures

Name	Morpholino sequences
Control (CTL)	CCT CTT ACC TCA GTT ACA ATT TAT A
H3	CGG TCT GTT TAG TAC GAG CCA TAG C
mut H3	CGc TCT cTT TAg TAC GAc CCA TAc C
H3.3	GGT CTG CTT TGT ACG GGC CAT TTC C
mut H3.3	GcT CTc CTT TcT ACG GGC gAT TaC C
HIRA	AGC TTC ATT GTC CCT CTG TGC CCA
mut HIRA	AGg TTg ATT GTC gCT CTc TGC aCA
p150	TAC TGC TGC TTC CTT CCC AGG CAT C
WDR5	CAT GGT GTC AGC ACT AGA ATG GTG C

We list the morpholinos sequences used in this study. The mutated nucleotides in mismatched morpholinos (mut MO) are shown in small letters.

Table S2: List of primers, related to Experimental procedures

Gene	Reference	Primers	
		Forward	*Reverse*
Sox2	Primer Express	CCATGCACCGCTATGATGTC	CTGCGAGCTGCTCATGGA
Otx2	Primer Express	AAGATTCAGGATTTAGCGCAAAA	TGCGCTCGCTCGGAATA
Sip1	Primer Express	CAGGCAGAGATCAGCACGAA	CTGTGCATTTGAACTTGCGATT
xBra	Primer Express	TGGCACCCAGAGAATGATCAC	CGGTCACTGCTATGAACTGTGTCT
BMP4	Primer Express	TCCTGCTCGGAGGCACTAAC	ACTTTCTTCTTGCCCGTGTCA
Myf5	Primer Express	TTCAGCGTCAGGTGGTTCAG	CCGCGGAAGGGAGTCAGT
MyoD	Primer Express	CAACCAAAGGCTCCCCAAA	GAGGCTCTCTATGTAGCGAATCG
ADMP	Primer Express	TCCAAACATCATCCGTTTTGC	CCAGCATGGGCTGTTTGC
Fgf8	Primer Express	CCTGGTGACCGACCAACTAAG	CCGGCTGTACAACTGGTAGGTT
Chordin	Primer Express	TGCAGTCAGATGGAGCAGGAT	TGCAGTCAGATGGAGCAGGAT
Zic3	Primer Express	TGCCAGCTCAGGGTACGAAT	CCTCACTGTTGGCAGAAACCA
xVent1	Primer Express	CCCAACAAATAAGCAAACTGGAA	CAGGTGCCCCCAGATATCTC
xVent2	Primer Express	CCAGAACCGCAGGATGAAAT	GGTATGAGTCTGGTCTGCCATCT
Noggin	Primer Express	CAGACCGGCTCCTAGTGAAAA	GGGATCCGGGTGCTCAAT
Goosecoid	Primer Express	TGTACCCTCAGCTACAGCATACG	GTGAGGCACTGGTGGAATCA
Derriere	Primer Express	GGATGGCAGAACTGGGTCAT	GGATGGCAGAACTGGGTCAT
Eomesodermin	Primer Express	TGACCCCCGTGCAACAA	TTTCGTAGGCCCCCATGTC
Siamois	Primer Express	GAGCCCAGGATACAGGTTTGG	TGGTTGCTCTTGGCAGATGTC
Sox17	Primer Express	CGCCAGCGACGATCAGA	GCCCGAGTCCAGTCATCATT
Cerberus	Primer Express	TGCAGTCAGATGGAGCAGGAT	TTCAGCGTCAGGTGGTTCAG
Endodermin	Primer Express	GACGGTGCGCAAATATTTCC	AGCGTTCCCATCAGCATCTG
Mixer	Primer Express	CCGCGGAAGGGAGTCAGT	CCGCGGAAGGGAGTCAGT
Xnr2	Primer Express	CCGCGGAAGGGAGTCAGT	CCGCGGAAGGGAGTCAGT
Mix1	Primer Express	TCAGCCATTTGCCATGAATC	TGGGATGCTGCTGGAAGTC
ODC	Primer Express	ACCCAGCCCTGGATAAATACTTC	TCCCAGGCTCTGCAATGATT
eFGF	(Casey et al., 1998)	CTTTCTTTCCAGAGAAACGACACCG	AACTCACGACTCCAACTTCCACTG
Wnt11	Primer 3	TGGAATGAGAGCGAACACTG	TCCAGCGCATGTCAGATAAG

We list the set of primers and their reference used for the RT-qPCRs.

SUPPLEMENTAL REFERENCES

Casey, E.S., O'Reilly, M.A., Conlon, F.L., and Smith, J.C. (1998). The T-box transcription factor Brachyury regulates expression of eFGF through binding to a non-palindromic response element. Development *125*, 3887-3894.

Kornberg, R.D., LaPointe, J.W., and Lorch, Y. (1989). Preparation of nucleosomes and chromatin. Methods Enzymol *170*, 3-14.

Nieuwkoop, P.D., and Faber, J. (1967). Normal Table of Xenopus laevis. Amsterdam: Daudin.

Quivy, J.P., Grandi, P., and Almouzni, G. (2001). Dimerization of the largest subunit of chromatin assembly factor 1: importance in vitro and during Xenopus early development. The EMBO journal *20*, 2015-2027.

Ray-Gallet, D., and Almouzni, G. (2004). DNA synthesis-dependent and -independent chromatin assembly pathways in Xenopus egg extracts. Methods Enzymol *375*, 117-131.

Ray-Gallet, D., Quivy, J.P., Scamps, C., Martini, E.M., Lipinski, M., and Almouzni, G. (2002). HIRA is critical for a nucleosome assembly pathway independent of DNA synthesis. Mol Cell *9*, 1091-1100.

Ray-Gallet, D., Quivy, J.P., Sillje, H.W., Nigg, E.A., and Almouzni, G. (2007). The histone chaperone Asf1 is dispensable for direct de novo histone deposition in Xenopus egg extracts. Chromosoma *116*, 487-496.

van der Heijden, G.W., Dieker, J.W., Derijck, A.A., Muller, S., Berden, J.H., Braat, D.D., van der Vlag, J., and de Boer, P. (2005). Asymmetry in histone H3 variants and lysine methylation between paternal and maternal chromatin of the early mouse zygote. Mech Dev *122*, 1008-1022.

Zernicka-Goetz, M., Pines, J., Ryan, K., Siemering, K.R., Haseloff, J., Evans, M.J., and Gurdon, J.B. (1996). An indelible lineage marker for Xenopus using a mutated green fluorescent protein. Development *122*, 3719-3724.

Zweidler, A. (1978). Resolution of histones by polyacrylamide gel electrophoresis in presence of nonionic detergents. Methods in cell biology *17*, 223-233.

Supplemental Figure 1

Click here to download high resolution image

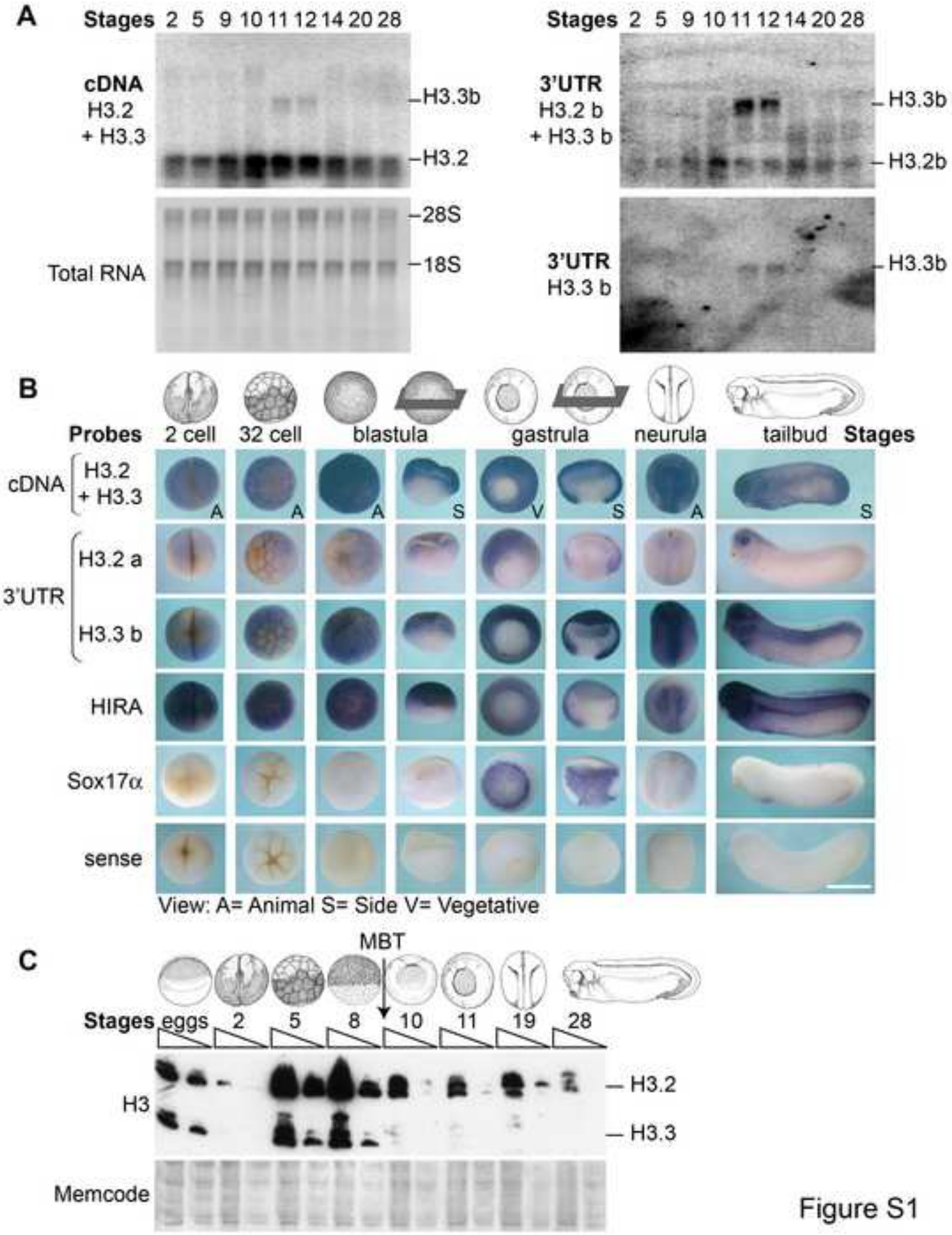

Figure S1

Supplemental Figure 2
Click here to download high resolution image

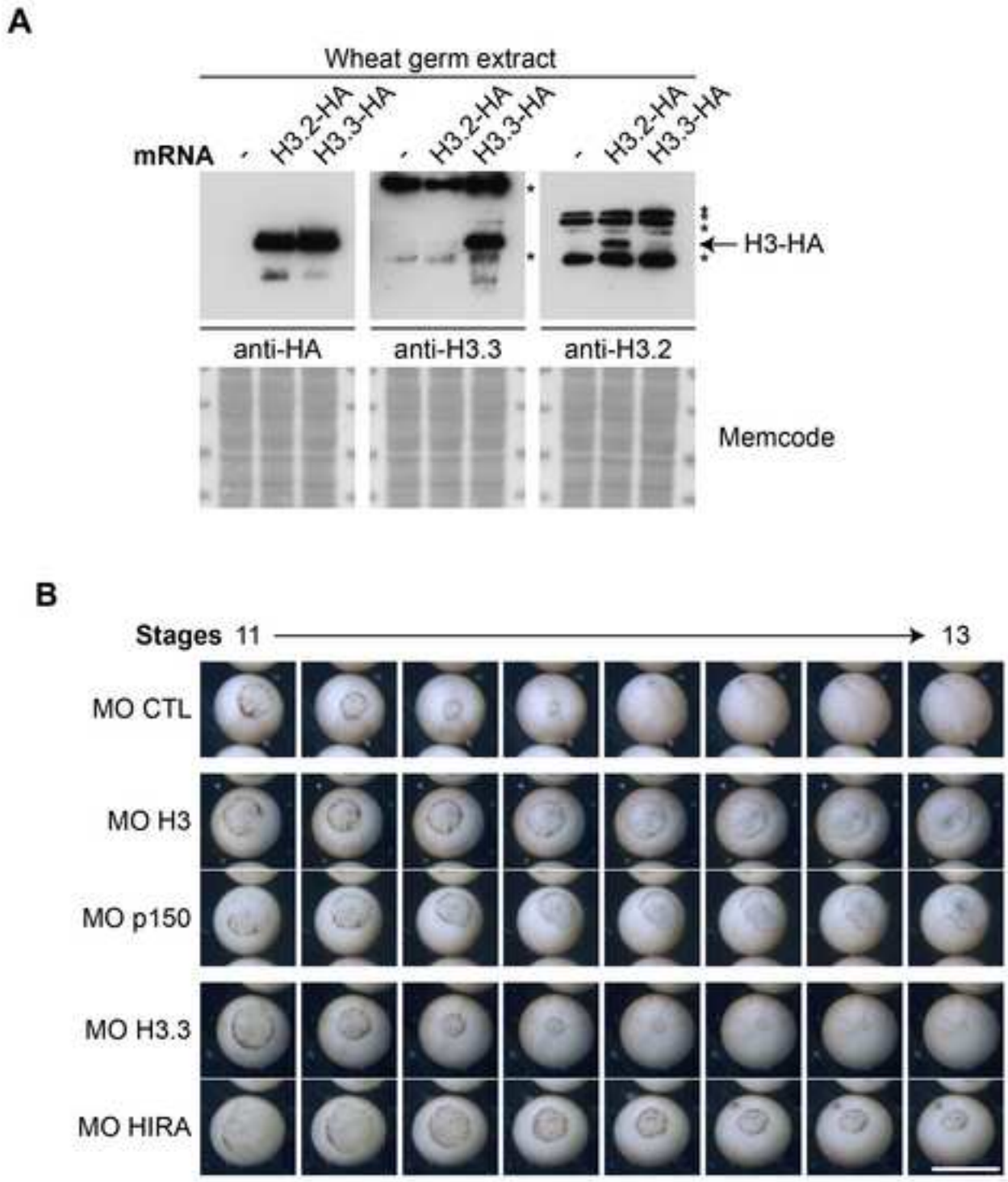

Figure S2

Supplemental Figure 3
Click here to download high resolution image

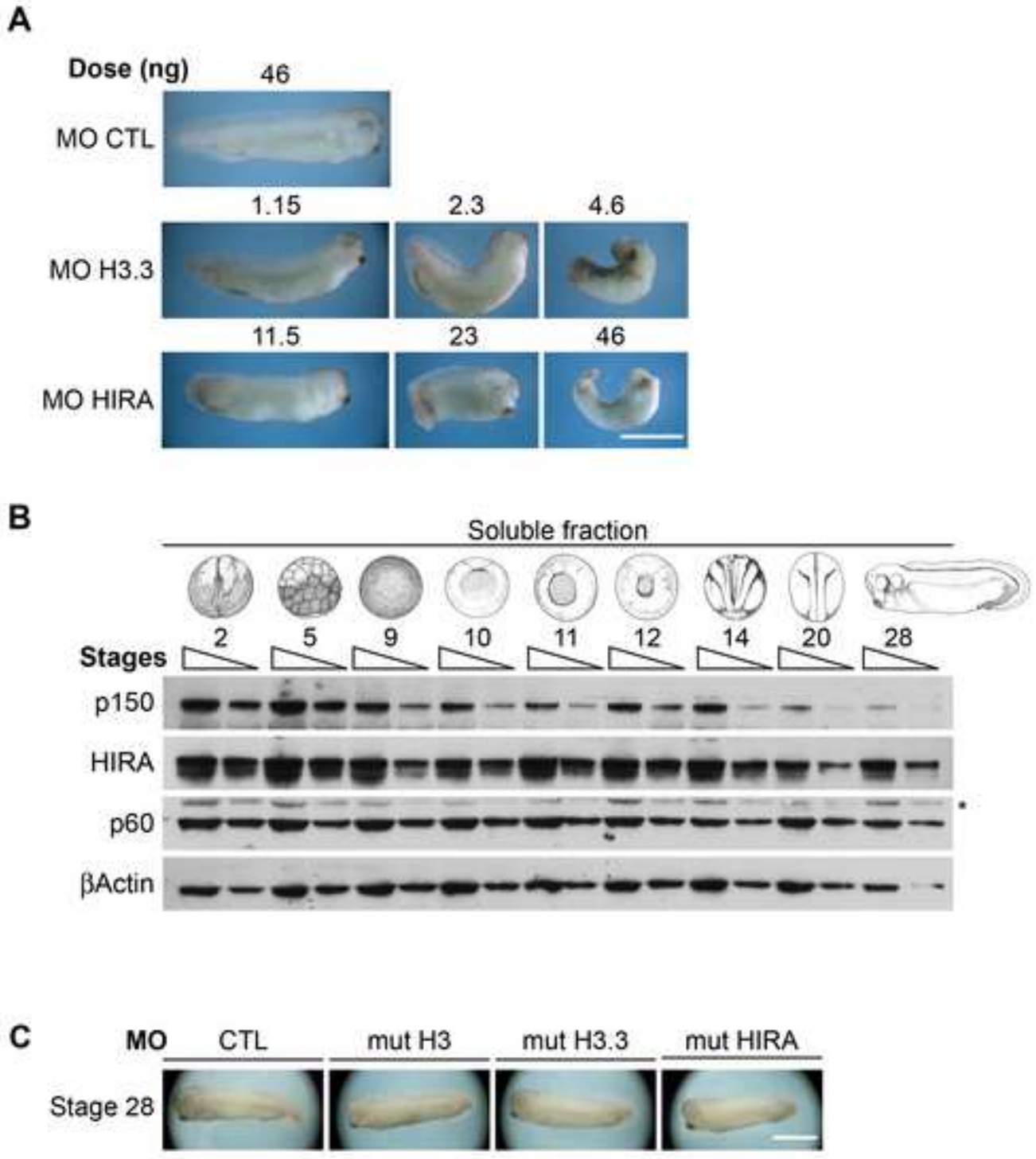

Figure S3

Supplemental Figure 4
Click here to download high resolution image

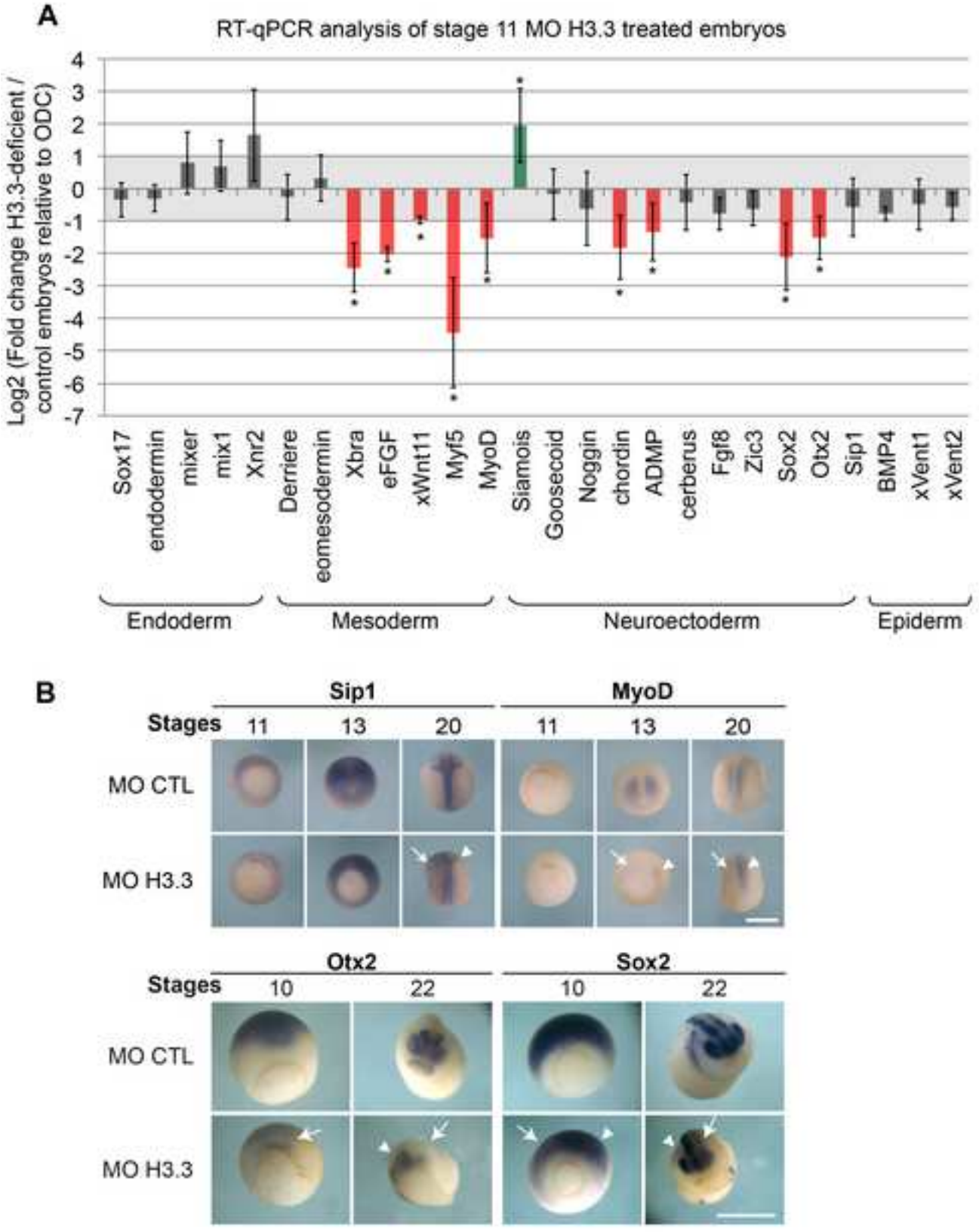

Figure S4

Supplemental Figure 5
Click here to download high resolution image

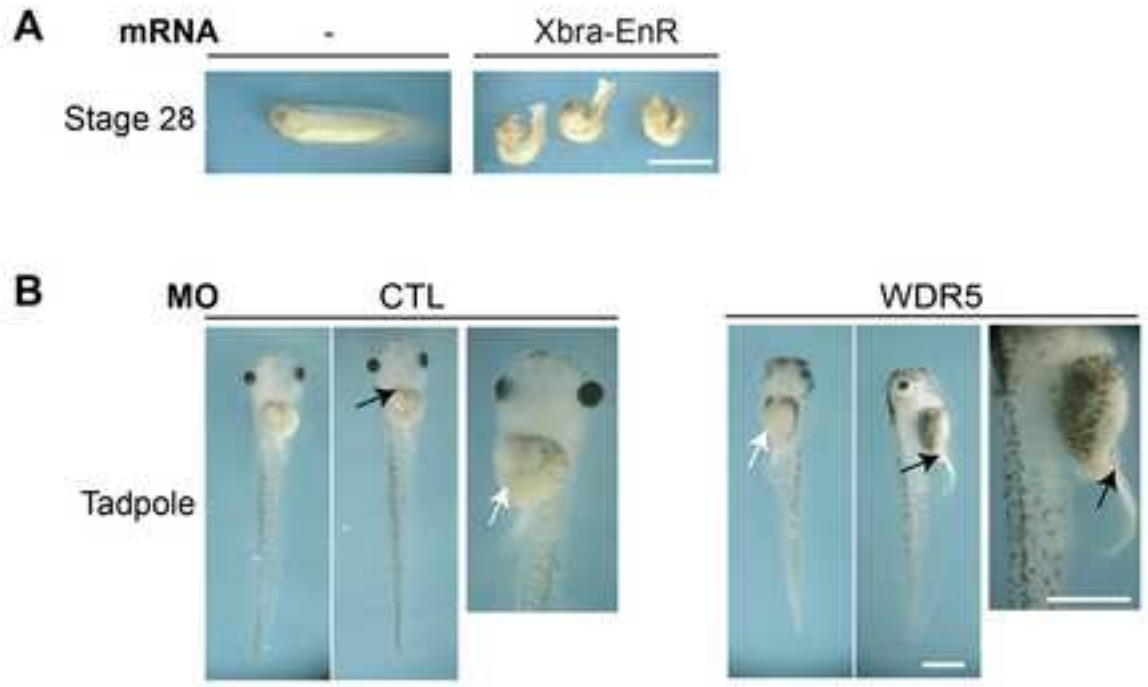

Figure S5

Supplemental Movie 1

Click here to download Supplemental Movies and Spreadsheets: Szenker Movie S1.mov

Supplemental Movie 2

Click here to download Supplemental Movies and Spreadsheets: Szenker Movie S2.mov